Pak.j.stat.oper.res. Vol.19 No. 3 2023 pp 491-519 DOI: http://dx.doi.org/10.18187/pjsor.v19i3.4089

Pakistan Journal of Statistics and Operation Research

A Novel Version of the Exponentiated Weibull Distribution: Copulas, Mathematical Properties and Statistical Modeling

Mohamed K. A. Refaie[1], Asmaa Ayoob Yaqoob[2], Mahmoud Ali Selim[3,4] and Emadeldin I. A. Ali[5,6]

* Corresponding Author

[1]Agami High Institute of Administrative Sciences, Alexandria, Egypt; refaie_top@yahoo.com

[2]Department of Statistics. College of Administration and Economics, University of Basrah, Iraq; asmaa.yaqoob@uobasrah.edu.iq

[3]Applied College, King Khalid University, KSA; Selim.one@gmail.com

[4]Department of Statistics, Faculty of Commerce, Al-Azhar University, Egypt.

[5]Department of Economics, College of Economics and Administrative Sciences, Al Imam Mohammad Ibn Saud Islamic University, Saudi Arabia; EIALI@IMAMU.EDU.SA

[6]Department of Mathematics, Statistics, and Insurance, Faculty of Business, Ain Shams University, Egypt; i_emadeldin@yahoo.com

Abstract

In this study, the authors of the current work describe a novel exponentiated Weibull distribution that they have invented. The study was written by the writers of the current work. It is required to analyze those properties once the pertinent mathematical properties have been derived. In addition to the dispersion index, the anticipated value, variance, skewness, and kurtosis are also statistically examined. The dispersion index is likewise examined. Other beneficial shapes that the new density can assume include "bathtub," "right skewed," "bimodal and left skewed," "unimodal and left skewed," and "bimodal and right skewed." Additionally, these forms can be merged to create a "bathtub." The term "bathtub (U-HRF)," "constant," "monotonically increasing," "upside down-increasing (reversed U-increasing)," "J-HRF," "upside down-constant," "increasing-constant," or "upside down (reversed U)" may be used to describe the new rate of failure. The greatest likelihood method's efficiency is assessed via graphical analysis. The main measures for this procedure's evaluation are biases and mean squared errors. The reader is given a scenario that graphically displays the adaptability and value of the innovative distribution through the use of three separate sets of actual data.

Keywords: Weibull Distribution; Rényi entropy index; Farlie Gumbel Morgenstern copula**;** Real Data Modeling; Hazard Function; Clayton copula.

1. Introduction

The exponentiated Weibull distribution, sometimes referred to as the EW distribution, is a significant distribution in the field of distribution theory. This is due to the fact that it can be adapted to a variety of situations and is quite versatile. Because it possesses a number of characteristics that make it suitable for modeling, it can be put to use in the process of modeling a diverse range of data sets and occurrences. The following is a list of some of the most important reasons why the EW distribution plays such an essential role in the field of distribution theory:

I. it applicable in a wide number of fields, The EW distribution provides a versatile framework for modeling lifetime data, which makes it possible for the modeling of lifetime data to be more flexible. Data of this kind may also be referred to as survival data in some contexts. It is capable of recording a wide variety of failure patterns, such as

those that are bathtub-shaped, increasing, decreasing, or maintaining constant in their severity. Its malleability makes such as reliability engineering, survival analysis, and actuarial science, amongst others.

II. The EW distribution has a flexible approach to modeling skewness and tail behavior, which enables it to describe data that is either positively or negatively skewed. This makes it possible for the distribution to model both positively and negatively skewed data. It is able to deal with a broad variety of skewness patterns, some of which include symmetric, right-skewed, and left-skewed distributions, amongst others. In addition, the EW distribution is able to take into consideration a wide range of tail behaviors, such as heavy-tailed and light-tailed distributions. This is one of the distribution's many benefits.

III. As a result of its adaptability and versatility, the EW distribution can be utilized in a wide range of different industries and fields of study. It has found uses in many different sectors, including engineering and finance, as well as the medical profession, environmental sciences, and examination of dependability. Because it is capable of simulating such a wide variety of data patterns and features, it is suitable for usage in a number of distinct settings.

IV. The estimation of the parameters of the EW distribution can be carried out in a variety of different ways, such as by making use of the maximum likelihood estimation or the method of moments. Both of these methods are examples of approaches that can be used. Both of these approaches come with a certain measure of adaptability. It is feasible to efficiently fit the distribution to the data that has been observed thanks to the adaptability of the method that is used to estimate the parameters.

V. Linking together with additional distribution networks The Weibull distribution with exponents is a flexible distribution that may be used to represent a variety of well-known distributions thanks to its use of special cases. This is due to the fact that the distribution uses the Weibull distribution as its foundation. For instance, the distribution can be simplified to a Weibull distribution when one of the shape parameters is set to the value 1. Depending on the values that are given for the parameters, it is also possible for it to decline to various distributions. Some examples of these distributions include the exponential, Rayleigh, gamma, and log-normal distributions. Its application is improved as a result of the fact that it is easy to connect it to other distributions, which also makes it feasible to simulate a broad variety of data types.

VI. The EW distribution gives a distributional form that may be tested against observed data using various tests that evaluate the degree to which the model is a good fit for the data. This can be accomplished by contrasting the data that was observed with the distributional form. These tests serve to determine whether or not the distribution adequately represents the patterns and attributes of the data, which is helpful for both the selection and validation of models. Additionally, these tests contribute to the determination of whether or not the distribution is appropriate.

VII. Because it possesses a number of mathematical qualities, the EW distribution may be approached analytically, which makes it more practicable. These characteristics add to the capability of analyzing the distribution as a whole. It enables the representation of several statistical measures in closed form, such as moments, quantiles, and reliability indices, amongst others. Because of these analytical capabilities, one's capacity to compute and analyze the characteristics of distributions can be done more quickly and easily.

VIII. The adaptability, diversity, and capability to be applied in a wide variety of circumstances that are all characteristics of the EW distribution all contribute to the acknowledgement of the relevance that the theory of distribution has received. Its analytical tractability and linkages to other distributions, as well as its ability to represent a variety of data patterns, skewness, and tail behavior, make it an excellent tool for modeling and analyzing a wide range of datasets and phenomena. In addition, its ability to model a variety of data patterns, skewness, and tail behavior, as well as its connections to other distributions, makes it an excellent tool.

The use of this distribution, which is regarded to be the most popular lifetime distribution model for modeling real lifespan data sets (see Murthy et al. (2004) and Rinne (2009)), has become more common in recent years. Rinne (2009) and Murthy et al. (2004) are two examples of authors who have used this model. The first generalization that allows for nonmonotone hazard rates is called the EW distribution (Mudholkar and Srivastava (1993). Cordeiro et al. (2017) converted the EW model to a new EW family of distributions. Yousof et al. (2017b) linked between the beta model and Weibull model and presented the Beta Weibull family. This distribution is also commonly referred to as the EW distribution. A random variable (RV) Y is said to have the EW distribution if the following equations can be used to determine its probability density function (PDF), cumulative distribution function (CDF), and hazard rate function (HRF):

$$h_{\theta,\delta}(y) = \theta\delta y^{\delta-1}e^{-y^{\delta}}\left(1-e^{-y^{\delta}}\right)^{\theta-1}, \tag{1}$$

$$H_{\theta,\delta}(y) = \left(1-e^{-y^{\delta}}\right)^{\theta}, \tag{2}$$

and

$$\tau_{\theta,\delta}(y) = \theta\delta y^{\delta-1}e^{-y^{\delta}}\frac{\left(1-e^{-y^{\delta}}\right)^{\theta-1}}{1-\left(1-e^{-y^{\delta}}\right)^{\theta}},$$

respectively, for $y > 0$, $\theta > 0$ and $\delta > 0$. For $\theta = 1$, the EW model reduces to we have the standard one parameter Weibull model (see Weibull (1951)). For $\delta = 2$, we have the exponentiated Rayleigh (ER) model also called the Burr type X model (Burr 1942). For $\delta = 1$, we have the exponentiated exponential (EE) model. For $\theta = \delta = 1$, we have the exponential (E) model. EW-H family of distributions is the term that has recently been given to a new family of distributions that was recently developed by Cordeiro et al. (2017). This new family of distributions was established by Refaie (2019) proposed and researched a new two-parameter EW model dubbed the Odd Lindley EW (OL-EW) model with features and applications to failure and survival times data sets. The model was given the name Odd Lindley EW (OL-EW). Using an extended Poisson-EW distribution, Refaie (2018) proposed a model that they referred to as the zero-truncated Poisson Topp Leone EW (ZTPTL-EW) model. Khalil et al. (2019) developed and investigated the Burr X EW model, also known as the BX-EW model. Characterizations, mathematical aspects, and applications to failure and survival time data were all incorporated in this model. generalized odd log-logistic EW (GOLL-EW) distribution with an application to the times of failure and running times for a sample of devices from a field-tracking study of a larger system by Mansour et al. (2020b). Mansour et al. (2020b) also included an application of this distribution to the times of failure and running times for the devices. The quasi-Poisson Burr type X EW (QPBX-EW) distribution, in addition to its copula, mathematical features, and applications, was presented by Mansour et al. (2020a).

In this work we introduce a new version of the EW distribution based on the odd Burr-G (OB-G) family (Alizadeh et al. (2017)). Due to Alizadeh et al. (2017), the CDF of the OB-G family is given by

$$F_{a,b,\underline{\xi}}(y) = 1 - \frac{\overline{H}_{\underline{\xi}}(y)^{ab}}{\left[H_{\underline{\xi}}(y)^{a} + \overline{H}_{\underline{\xi}}(y)^{a}\right]^{b}}, \tag{3}$$

where $\overline{H}_{\underline{\xi}}(y) = 1 - H_{\underline{\xi}}(y)$ refers to the survival function (SF) of any baseline model. The PDF corresponding to (3) is given by

$$f_{a,b,\underline{\xi}}(y) = abh_{\underline{\xi}}(y)H_{\underline{\xi}}(y)^{a-1}\frac{\overline{H}_{\underline{\xi}}(y)^{ab-1}}{\left[H_{\underline{\xi}}(y)^{a} + \overline{H}_{\underline{\xi}}(y)^{a}\right]^{1+b}}. \tag{4}$$

According to Gleaton and Lynch (2006), the OB-G family shrinks to the Odd G (O-G) family when b=1. The proportional reversed hazard rate family (PRHR) is the result of the OB-G family when a=1 (see Gupta and Gupta 2007). In this work, we develop and investigate the odd Burr EW (OB-EW) model, a new EW model based on the OB-G family. When (2) is inserted into (4), the CDF of OB-EW can be expressed as

$$F_{\underline{V}}(y) = 1 - \frac{\left[1-\left(1-e^{-y^{\delta}}\right)^{\theta}\right]^{ab}}{\left\{\left(1-e^{-y^{\delta}}\right)^{\theta a} + \left[1-\left(1-e^{-y^{\delta}}\right)^{\theta}\right]^{a}\right\}^{b}}, \tag{5}$$

where $S_{\underline{V}}(y) = 1 - F_{\underline{V}}(y)|_{(\underline{V}=a,b,\theta,\delta)}$. For $b = 1$, the OB-EW reduces to the O-EW model. For $a = 1$, the OB-EW model reduces to the PRHR-EW. The PDF corresponding to (5) is given by

$$f_{\underline{V}}(y) = ab\theta\delta y^{\delta-1}e^{-y^{\delta}}\frac{\left(1-e^{-y^{\delta}}\right)^{\theta a-1}\left[1-\left(1-e^{-y^{\delta}}\right)^{\theta}\right]^{ab-1}}{\left\{\left(1-e^{-y^{\delta}}\right)^{\theta a} + \left[1-\left(1-e^{-y^{\delta}}\right)^{\theta}\right]^{a}\right\}^{b+1}}. \tag{6}$$

The hazard rate function (HRF) for the new model can be get from $f_{\underline{V}}(y)/S_{\underline{V}}(y)$. Let $c = inf\left\{y|_{H_{\underline{\xi}}(y)>0}\right\}$, the asymptotics of the CDF, PDF and HRF as $y \to 0$ are given by

$$F_{\underline{V}}(y|_{(y\to 0)}) \sim b\left(1-e^{-y^{\delta}}\right)^{\theta a}, f_{\underline{V}}(y|_{(y\to 0)}) \sim ab\theta\delta y^{\delta-1}e^{-y^{\delta}}\left(1-e^{-y^{\delta}}\right)^{\theta a-1},$$

and

$$h_{\underline{V}}(y|_{(y\to 0)}) \sim ab\theta\delta y^{\delta-1}e^{-y^{\delta}}\left(1-e^{-y^{\delta}}\right)^{\theta a-1}$$

The asymptotics of CDF, PDF and HRF as $y \to \infty$ are given by

$$1-F_{\underline{V}}(y|_{(y\to\infty)}) \sim a^{b}\left\{1-\left(1-e^{-y^{\delta}}\right)^{\theta}\right\}^{b}, f_{\underline{V}}(y|_{(y\to\infty)}) \sim a^{b}b\theta\delta\frac{y^{\delta-1}e^{-y^{\delta}}\left(1-e^{-y^{\delta}}\right)^{\theta-1}}{\left\{1-\left(1-e^{-y^{\delta}}\right)^{\theta}\right\}^{1-b}},$$

and

$$h_{\underline{V}}(y|_{(y\to\infty)}) \sim b\theta\delta\frac{y^{\delta-1}e^{-y^{\delta}}\left(1-e^{-y^{\delta}}\right)^{\theta-1}}{1-\left(1-e^{-y^{\delta}}\right)^{\theta}}.$$

For simulation of this new model, we obtain the quantile function (QF) of y (by inverting (5)), say $y_{\mathcal{W}} = F^{-1}(\mathcal{W})$, as

$$y_{\mathcal{W}} = \left[-ln\left(1-\left\{\frac{\left[1-(1-\mathcal{W})^{\frac{1}{b}}\right]^{\frac{1}{a}}}{(1-\mathcal{W})^{\frac{1}{ab}}+\left[1-(1-\mathcal{W})^{\frac{1}{b}}\right]^{\frac{1}{a}}}\right\}^{\frac{1}{\theta}}\right)\right]^{\frac{1}{\delta}}. \quad (7)$$

Equation (7) is utilized so that the new model can be modeled accurately.

Exploring the shape of the PDF and the HRF in statistical analysis offers valuable insights into the behavior and characteristics of a distribution. Here's why studying these aspects is statistically important:

I. The shape of the PDF provides information about the distribution's central tendency, variability, skewness, and kurtosis. Analyzing these properties helps in understanding how data points are distributed within the distribution and whether it fits the underlying assumptions of the Exponentiated Weibull Distribution.

II. Comparing the shape of the PDF of the OB-EW model with other distributions allows for model selection. If the PDF closely matches the data's distributional characteristics, it suggests that the Exponentiated Weibull Distribution is a suitable choice for modeling the data.

III. Different shapes of PDFs indicate variations in the distribution's parameters. By examining the shape, you can gain insights into the impact of parameter changes on the distribution. This can aid in interpreting the parameters in the context of the real-world phenomenon being modeled.

IV. The hazard rate function is fundamental in survival analysis and reliability engineering. It provides information about the conditional probability of an event occurring at a specific time given that it has not occurred until that time. Analyzing the hazard rate function helps identify periods of higher risk or vulnerability, which is crucial in many applications.

V. Understanding the hazard rate function's shape can inform risk assessments and guide decision-making processes. For instance, in healthcare, analyzing the hazard rate function could help healthcare providers determine optimal treatment strategies based on the patient's risk profile.

VI. When comparing multiple distributions, examining the shapes of their hazard rate functions can reveal important differences in their failure patterns, which can influence the choice of distribution for modeling specific data types.

VII. The shape of the hazard rate function provides insights into how well the OB-EW model fits real-world survival or reliability data. If the observed hazard rates deviate significantly from the distribution's expected hazard rates, it might indicate model misspecification or the presence of hidden patterns in the data.

VIII. The shape of the hazard rate function influences predictions about future events. Understanding how changes in the distribution's parameters affect the hazard rate can help in making more accurate predictions about event occurrences.

IX. Unusual shapes in the PDF or hazard rate function could be indicative of outliers or anomalous behavior in the data. Investigating these cases can provide insights into unusual events or system failures.

In summary, exploring the shape of the probability density function and the hazard rate function plays a pivotal role in understanding the distribution's behavior, its suitability for modeling, and its applications in various fields. It also supports robust statistical analysis, model validation, and informed decision-making. The new PDF can be seen in a variety of displays scattered around Figure 1. Figure 1 displays the newly developed HRF using multiple different chart types. As can be seen in Figure 1, the new PDF can either have a "unimodal" distribution or a "bimodal" distribution with right and left skewed densities. The statistics displayed in that graphic served as the foundation for this information. According to Figure 2, it is indicated that the new HRF can take the form of a "bathtub (U-HRF)", "constant", "increasing", "upside down-increasing (reversed U-increasing)", "J-HRF", "upside down-constant", "decreasing", "increasing-constant", or "upside down (reversed U)".

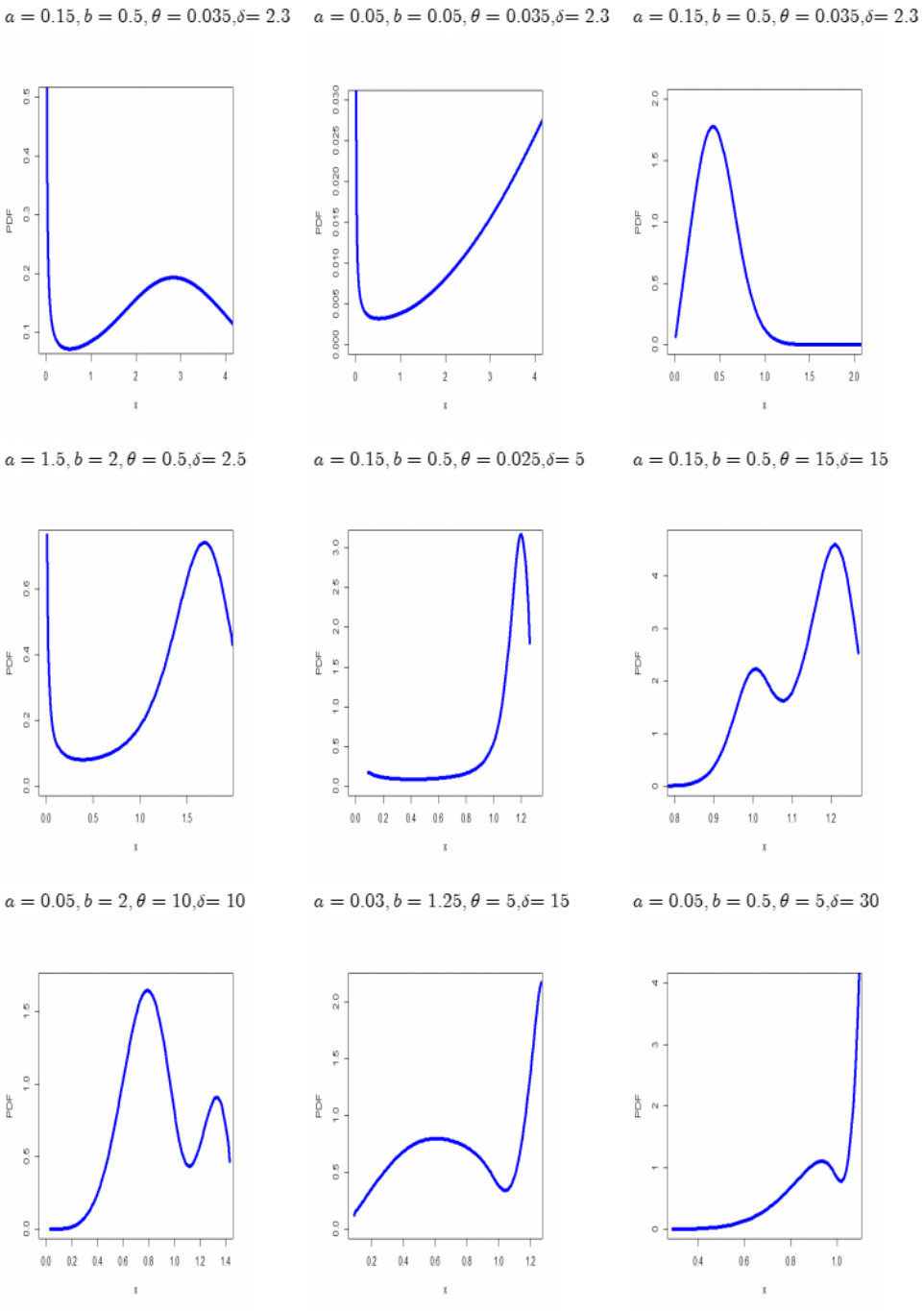

Figure 1: Different plots for the new density.

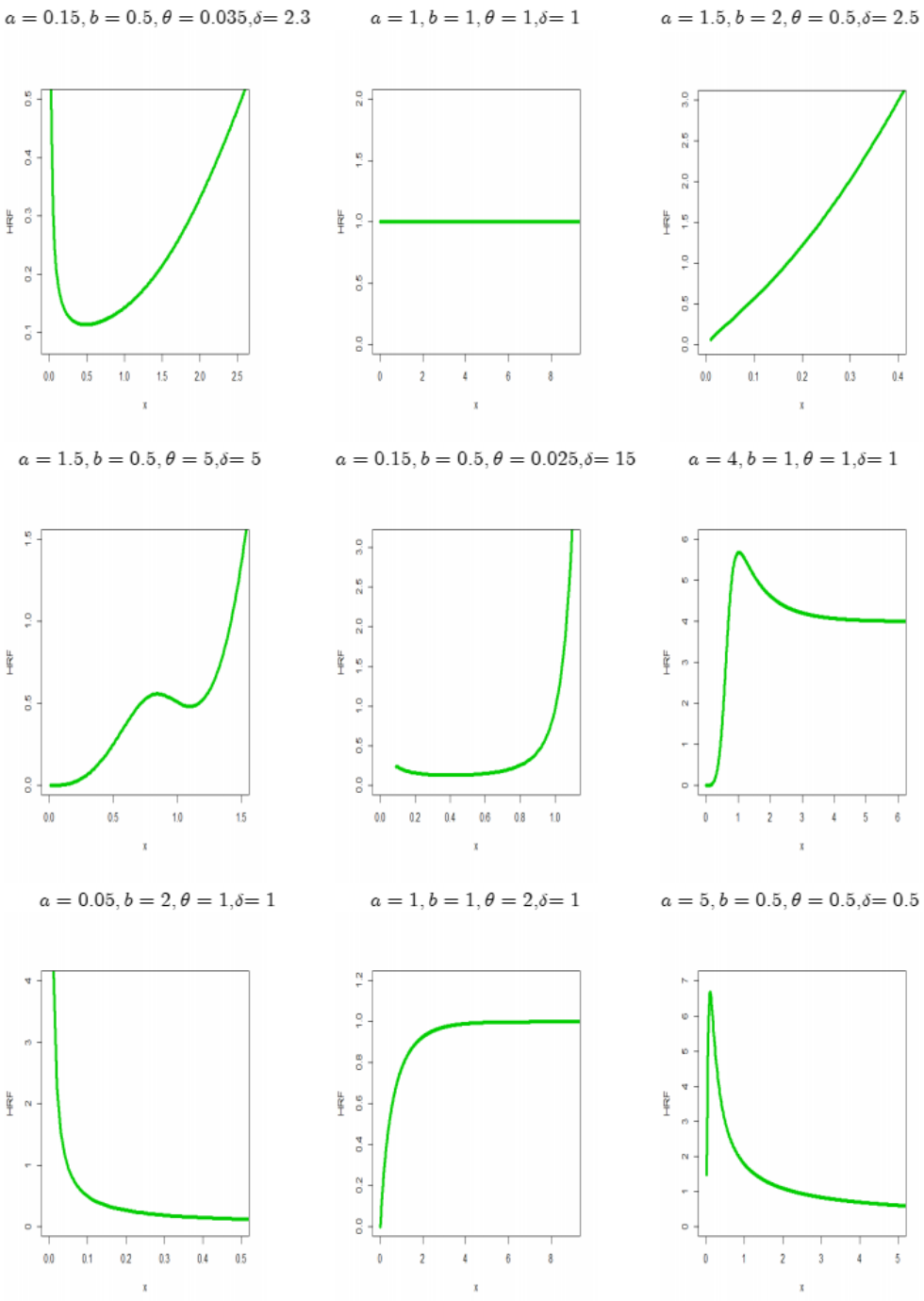

Figure 2: Different plots for the new HRF.

2. Bivariate versions via copula

A copula is a multivariate CDF that is defined in the field of probability theory by the condition that the marginal probability distribution of each variable is uniform on the interval [0,1]. With the assistance of a piece of software known as a copula, one is able to gain an understanding of the interdependence of random variables. Using copulas in modeling bivariate and multivariate data offers several advantages, which are particularly relevant in capturing complex dependencies between variables. Here are the main advantages of using copulas in this context:

I. Copula provides a flexible framework for modeling dependence between variables. Unlike parametric approaches that assume specific forms of dependence (e.g., linear or Gaussian), copulas allow for more

general and flexible modeling of complex dependence structures. This flexibility is crucial when dealing with real-life data that often exhibit nonlinear and non-Gaussian dependencies.

II. Copulas allow for the separation of modeling marginal distributions from the modeling of the dependence structure. This means that the marginal distributions of each variable can be modeled individually, taking into account their specific characteristics and data properties. This separation simplifies the modeling process by focusing on capturing the joint dependence structure, which can be more challenging to specify accurately.

III. Copulas can capture a wide range of dependence structures, including linear, nonlinear, and tail dependence. This flexibility is important in capturing different types of dependencies observed in real-life data. Copulas can model symmetric or asymmetric dependencies, long-range dependencies, and the presence of extreme events (tail dependence) accurately.

IV. Copulas provide efficient estimation methods for both parametric and nonparametric models. Parametric copulas specify a functional form, and their parameters can be estimated using maximum likelihood estimation or other estimation techniques. Nonparametric copulas, such as vine copulas, offer more flexibility by allowing local modeling of dependence structures. Estimation methods for copulas are well-established and computationally efficient.

V. Copulas can handle mixed data types, including continuous, discrete, and categorical variables. By transforming each variable into a uniform distribution using marginal transformations, copulas can model the joint dependence structure regardless of the specific data type. This makes copulas suitable for analyzing complex datasets that include different types of variables.

VI. Copulas enable efficient simulation of dependent variables from specified marginal distributions and dependence structure. This is valuable for generating synthetic data for risk analysis, portfolio optimization, stress testing, and Monte Carlo simulations. Copulas can also provide reliable estimates of joint probabilities and quantiles, which are essential for risk management and decision-making in various domains.

VII. Copulas offer various diagnostic tools and goodness-of-fit tests to assess the adequacy of the chosen copula model. These tests help evaluate how well the copula captures the observed dependence structure in the data. If the copula model does not fit the data well, alternative copula families or modifications can be explored.

In summary, copulas provide a flexible and powerful framework for modeling complex dependence structures in bivariate and multivariate data. Their flexibility in modeling dependence, separation of marginal distributions and dependence structure, ability to capture various dependency types, and efficient estimation methods make them valuable in diverse fields such as finance, insurance, risk management, and environmental sciences. In this Section, we derive some new bivariate OB-EW (B-OB-EW) type distributions using Farlie Gumbel Morgenstern (FGM) copula (see Morgenstern (1956), Gumbel (1958), Gumbel (1960), Johnson and Kotz (1975) and Johnson and Kotz (1977)), modified FGM copula (see Rodriguez-Lallena and Ubeda-Flores (2004)), Clayton copula, Renyi's entropy (Pougaza and Djafari (2011)) and Ali-Mikhail-Haq copula (Ali et al. (1987)). The Multivariate OB-EW (M-OB-EW) type is also presented.

On the other hand, future efforts can concentrate on the investigation of these novel models. Let's begin by taking a look at the combined CDF of the members of the FGM family, where

$$H_{\varsigma}(\mathcal{W},\mathcal{S}) = \mathcal{W}\mathcal{S}(1+\varsigma\mathcal{W}^{\bullet}\mathcal{S}^{\bullet})|_{\mathcal{W}^{\bullet}=1-\mathcal{W},\mathcal{S}^{\bullet}=1-\mathcal{S}},$$

and the marginal function $\mathcal{W}=F_1$, $\mathcal{S}=F_2$, $\varsigma\in(-1,1)$ is a dependence parameter and for every $\mathcal{W},\mathcal{S}\in(0,1)$, $H(\mathcal{W},0)=H(0,\mathcal{S})=0$ which is "grounded minimum" and $H(\mathcal{W},1)=\mathcal{W}$ and $H(1,\mathcal{S})=\mathcal{S}$ which is "grounded maximum", $H(\mathcal{W}_1,\mathcal{S}_1)+H(\mathcal{W}_2,\mathcal{S}_2)-H(\mathcal{W}_1,\mathcal{S}_2)-H(\mathcal{W}_2,\mathcal{S}_1)\geq 0$.

2.1 FGM copula

A copula is continuous in $\mathcal{W}$ and $\mathcal{S}$; actually, it satisfies the stronger Lipschitz condition, where

$$|H(\mathcal{W}_2,\mathcal{S}_2)-H(\mathcal{W}_1,\mathcal{S}_1)|\leq|\mathcal{W}_2-\mathcal{W}_1|+|\mathcal{S}_2-\mathcal{S}_1|.$$

For $0\leq\mathcal{W}_1\leq\mathcal{W}_2\leq 1$ and $0\leq\mathcal{S}_1\leq\mathcal{S}_2\leq 1$, we have

$$Pr(\mathcal{W}_1\leq\mathcal{W}\leq\mathcal{W}_2,\mathcal{S}_1\leq\mathcal{S}\leq\mathcal{S}_2)=H(\mathcal{W}_1,\mathcal{S}_1)+H(\mathcal{W}_2,\mathcal{S}_2)-H(\mathcal{W}_1,\mathcal{S}_2)-H(\mathcal{W}_2,\mathcal{S}_1)\geq 0.$$

Then, setting $\mathcal{W}^{\bullet} = 1 - F_{\underline{V_1}}(y_1)|_{[\mathcal{W}^{\bullet}=(1-\mathcal{W})\in(0,1)]}$ and $\mathcal{S}^{\bullet} = 1 - F_{\underline{V_2}}(y_2)|_{[\mathcal{S}^{\bullet}=(1-\mathcal{S})\in(0,1)]}$, we can esaily obtain the joint CDF of the OB-EW using the FGM family. The joint PDF can then be derived from $c_{\varsigma}(\mathcal{W},\mathcal{S}) = 1 + \varsigma\mathcal{W}^{\bullet}\mathcal{S}^{\bullet}|_{(\mathcal{W}^{\bullet}=1-2\mathcal{W} \text{ and } \mathcal{S}^{\bullet}=1-2\mathcal{S})}$ or from $c_{\varsigma}(\mathcal{W},\mathcal{S}) = f(y_1,y_2) = H(F_1,F_2)f_1f_2$.

2.2 Modified FGM copula

The modified FGM copula is defined as $H_{\varsigma}(\mathcal{W},\mathcal{S}) = \mathcal{W}\mathcal{S}[1 + \varsigma D(\mathcal{W})C(\mathcal{S})]|_{\varsigma\in(-1,1)}$ or $H_{\varsigma}(\mathcal{W},\mathcal{S}) = \mathcal{W}\mathcal{S} + \varsigma A_{\mathcal{W}}B_{\mathcal{S}}|_{\varsigma\in(-1,1)}$, where $A_{\mathcal{W}} = \mathcal{W}D(\mathcal{W})$, and $B_{\mathcal{S}} = \mathcal{S}C(\mathcal{S})$ and $D(\mathcal{W})$ and $C(\mathcal{S})$ are two continuous functions on $(0,1)$ with $D(0) = D(1) = C(0) = C(1) = 0$. Let

$$c_1(A_{\mathcal{W}}) = inf\left\{A_{\mathcal{W}} \ : \ \frac{\partial}{\partial\mathcal{W}}A_{\mathcal{W}}\right\}|_{\omega_{1,\mathcal{W}}} < 0, c_2(A_{\mathcal{W}}) = s\mathcal{W}p\left\{A_{\mathcal{W}} \ : \ \frac{\partial}{\partial\mathcal{W}}A_{\mathcal{W}}\right\}|_{\omega_{1,\mathcal{W}}} < 0,$$

$$d_1(B_{\mathcal{S}}) = inf\left\{B_{\mathcal{S}} \ : \ \frac{\partial}{\partial\mathcal{S}}B_{\mathcal{S}}\right\}|_{\omega_{2,\mathcal{S}}} > 0, d_2(B_{\mathcal{S}}) = s\mathcal{W}p\left\{B_{\mathcal{S}} \ : \ \frac{\partial}{\partial\mathcal{S}}B_{\mathcal{S}}\right\}|_{\omega_{2,\mathcal{S}}} > 0.$$

Then, $1 \le min\{c_1(A_{\mathcal{W}})c_2(A_{\mathcal{W}}), d_1(B_{\mathcal{S}})d_2(B_{\mathcal{S}})\} < \infty$ where

$$\mathcal{W}\frac{\partial}{\partial\mathcal{W}}D(\mathcal{W}) = \frac{\partial}{\partial\mathcal{W}}A_{\mathcal{W}} - D(\mathcal{W}),$$

$$\omega_{1,\mathcal{W}} = \left\{\mathcal{W} \ : \ \mathcal{W}\in(0,1)|_{\frac{\partial}{\partial\mathcal{W}}A_{\mathcal{W}} \text{ exists}}\right\} \text{ and } \omega_{2,\mathcal{S}} = \left\{\mathcal{S} \ : \ \mathcal{S}\in(0,1)|_{\frac{\partial}{\partial\mathcal{S}}B_{\mathcal{S}} \text{ exists}}\right\}.$$

Type-I:

Consider the following functional form for both $D(\mathcal{W})$ and $C(\mathcal{S})$. Then, the B-OB-EW-FGM (Type-**I**) can be derived from

$$H_{\varsigma}(\mathcal{W},\mathcal{S}) = \mathcal{W}\mathcal{S}(1 + \varsigma\mathcal{W}^{\bullet}\mathcal{S}^{\bullet}).$$

Type-II:

Let $D(\mathcal{W})^{\bullet}$ and $C(\mathcal{S})^{\bullet}$ be two functional form satisfying all the conditions stated earlier where $D(\mathcal{W})^{\bullet}|_{(\varsigma_1>0)} = \mathcal{W}^{\varsigma_1}(1-\mathcal{W})^{1-\varsigma_1}$ and $C(\mathcal{S})^{\bullet}|_{(\varsigma_2>0)} = \mathcal{S}^{\varsigma_2}(1-\mathcal{S})^{1-\varsigma_2}$. Then, the corresponding B-OB-EW-FGM **(**Type-**II)** can be derived from

$$H_{\varsigma,\varsigma_1,\varsigma_2}(\mathcal{W},\mathcal{S}) = \mathcal{W}\mathcal{S}[1 + \varsigma D(\mathcal{W})^{\bullet}\, C(\mathcal{S})^{\bullet}].$$

Type-III:

Let $\overline{D^{\bullet}(\mathcal{W})} = \mathcal{W}[log(1+\mathcal{W}^{\bullet})]$ and $\overline{C^{\bullet}(\mathcal{S})} = \mathcal{S}[log(1+\mathcal{S}^{\bullet})]$ for all $D(\mathcal{W})$ and $C(\mathcal{S})$ which satisfy all the conditions stated earlier. In this case, one can also derive a closed form expression for the associated CDF of the B-OB-EW-FGM (Type-**III**) from

$$H_{\varsigma}(\mathcal{W},\mathcal{S}) = \mathcal{W}\mathcal{S}\left(1 + \varsigma\overline{D^{\bullet}(\mathcal{W})}\,\overline{C^{\bullet}(\mathcal{S})}\right).$$

2.3 Clayton copula

The Clayton copula can be considered as $H(\mathcal{S}_1,\mathcal{S}_2) = [(1/\mathcal{S}_1)^{\varsigma} + (1/\mathcal{S}_2)^{\varsigma} - 1]^{-\varsigma^{-1}}|_{\varsigma\in(0,\infty)}$. Setting $\mathcal{S}_1 = F_{\underline{V_1}}(\mathcal{W})$ and $\mathcal{S}_2 = F_{\underline{V_2}}(y)$, the B-OB-EW type can be derived from $H(\mathcal{S}_1,\mathcal{S}_2) = H(F_{\underline{V_1}}(\mathcal{S}_1), F_{\underline{V_1}}(\mathcal{S}_2))$. Similarly, the M-OB-EW can be derived from

$$H(\mathcal{S}_k) = \left(\sum_{k=1}^{d}\mathcal{S}_k^{-\varsigma} + 1 - d\right)^{-\varsigma^{-1}}.$$

2.4 Renyi's entropy copula

Using the theorem of Pougaza and Djafari (2011), the associated B-OB-EW can be derived from $H(\mathcal{W},\mathcal{S}) = y_2\mathcal{W} + y_1\mathcal{S} - y_1y_2$.

2.5 Ali-Mikhail-Haq copula

The Ali-Mikhail-Haq (AMH) copula is a bivariate copula model that was proposed by Ali, Mikhail, and Haq in 1978. It is also known as the AMH-2 copula or the squashed Gaussian copula. The AMH copula is a parametric copula that assumes a particular functional form for the dependence structure between two random variables. The AMH copula is derived from the standard Gaussian copula by transforming the standard normal marginals to non-standard marginals. The transformation introduces a parameter called the squashing parameter (θ) that controls the strength of dependence and the tail behavior of the copula. The AMH copula has been used in various applications, such as

finance, risk management, and insurance. It allows for the modeling of both positive and negative tail dependence, which is important for capturing extreme events and accurately estimating risk measures. It's worth noting that while the AMH copula has some desirable properties, it may not capture all types of dependence structures observed in real-life data. Depending on the specific characteristics of the data, other copula models or nonparametric approaches may be more appropriate. The choice of copula model should be based on careful consideration of the data properties and the research objectives.

Under the stronger Lipschitz condition and for any $\mathcal{W}^{\bullet} = 1 - F_{\underline{V_1}}(h_1)|_{[\mathcal{W}^{\bullet}=(1-\mathcal{W})\in(0,1)]}$ and $\mathcal{S}^{\bullet} = 1 - F_{\underline{V_2}}(h_2)|_{[\mathcal{S}^{\bullet}=(1-\mathcal{S})\in(0,1)]}$, the Archimedean Ali--Mikhail-Haq copula can expressed as

$$H(\mathcal{W},\mathcal{S}) = \mathcal{W}\mathcal{S}[1-\varsigma\mathcal{W}^{\bullet}\mathcal{S}^{\bullet}]^{-1}|_{\tau\in(-1,1)}.$$

Here are some examples of its applications:

I. The AMH copula is used to model the dependence between different risks in insurance portfolios. It allows for capturing tail dependence, which is crucial for estimating the joint probability of extreme events. The copula can be employed in the calculation of aggregate risk measures, such as Value-at-Risk (VaR) and Conditional Tail Expectation (CTE), for assessing and managing risk in insurance and reinsurance industries.

II. In finance, the AMH copula is utilized for modeling the dependence between different financial assets in portfolio optimization. By capturing both positive and negative tail dependence, the copula can provide a more accurate estimation of risk and diversification benefits. It helps investors and portfolio managers make informed decisions regarding asset allocation and risk management strategies.

III. The AMH copula is applied in credit risk modeling to capture the dependence between default events of different borrowers or counterparties. By incorporating tail dependence, the copula enables a more accurate assessment of credit portfolio risk and the estimation of credit risk measures, such as the probability of default (PD) and the loss given default (LGD). It aids in credit portfolio stress testing and the evaluation of credit risk concentrations.

IV. Copula models, including the AMH copula, are used to analyze the dependence between different environmental variables. For example, in hydrology, the copula can capture the joint behavior of rainfall and streamflow, allowing for the assessment of flood risks, water resource management, and hydrological modeling.

V. The AMH copula finds applications in actuarial science for modeling the dependence between different insurance-related variables, such as claim amounts and claim frequencies. It assists in estimating aggregated claim distributions and evaluating the potential impact of correlated risks on insurance portfolios.

VI. The AMH copula can be used in reliability engineering to model the dependence between the failure times of different components or systems. By capturing tail dependence, it helps in analyzing system reliability, assessing the risk of system failures, and optimizing maintenance strategies.

3. Mathematical properties

In many areas, including statistics, data analysis, machine learning, and risk assessment, it is crucial to understand the mathematical features of probability distributions. Reasons why it's critical to comprehend these qualities include the following:

I. A formal foundation for modeling uncertainty is provided by probability distributions. We can understand the behavior of random variables and estimate the likelihood of various events by looking at their mathematical features. This enables us to analyze data effectively and draw conclusions that are useful.

II. Probability distributions are used to mathematically depict real-life occurrences when describing data. They enable us to succinctly describe and summarize data. In order to more accurately represent and analyze data, we can determine which distribution best matches a specific dataset by examining its attributes.

III. Probability distributions are essential to both statistical inference and parameter estimation. We can create effective estimating methods, carry out hypothesis testing, build confidence intervals, and make predictions based on observable data by comprehending their mathematical aspects.

IV. Probability distributions are frequently employed in simulations and optimization techniques. We can create random samples that simulate real-life processes by examining their attributes, and we can run

Monte Carlo simulations to assess complex systems. Furthermore, understanding distribution features might aid in creating effective methods for solving optimization problems.

V. Probability distributions aid in risk assessment and management during decision-making. We can calculate the likelihood of alternative outcomes and assess the possible effects of uncertain events by studying the characteristics of distinct distributions. This information is essential for making decisions in uncertain situations, such as those involving insurance, quality control, and financial planning.

VI. Probability distributions play a crucial role in the processes of model selection and validation. We can evaluate the goodness-of-fit and select the best model by comparing observed data with several distributional hypotheses. Understanding distributional features makes it easier to spot assumptions that are not being met and to spot areas where models should be improved.

3.1 Useful representations

Alizadeh et al. (2017) have allowed us to express the PDF in (6) as follows:

$$f(y) = \sum_{j=0}^{\infty} \nabla_j h_{\theta^\bullet}(y)|_{(\theta^\bullet = \theta(1+j))}, \tag{8}$$

where

$$\nabla_j = \frac{ab}{1+j} \sum_{\zeta_1,\zeta_2=0}^{\infty} \sum_{\zeta_3=j}^{\infty} (-1)^{\zeta_2+k+j} \binom{-(1+b)}{\zeta_1} \binom{-[a(1+\zeta_1)+1]}{\zeta_2} \binom{a(1+\zeta_1)+\zeta_2+1}{\zeta_3} \binom{\zeta_3}{j},$$

and $\pi_{\theta^\bullet}(y)$ is the PDF of the EW model with power parameter $\theta^\bullet$. By integrating Equation (8), the CDF of y becomes

$$F(y) = \sum_{j=0}^{\infty} \nabla_j \Pi_{\theta^\bullet}(y), \tag{9}$$

where $\Pi_{\theta^\bullet}(y)$ is the CDF of the EW distribution with power parameter $\theta^\bullet$.

3.2 Moments and incomplete moments

The r^{th} ordinary moment of Y is given by $\mu'_{r,Y} = E(y^r) = \int_{-\infty}^{\infty} y^r f(y) dy$ then we obtain

$$\mu'_{r,Y}|_{(r>-\delta)} = b^r \Gamma(1 + r\delta^{-1}) \sum_{j,h=0}^{\infty} \nabla_{j,h}^{(r,\theta(1+j))}, \tag{10}$$

where

$$\nabla_{j,h}^{(r,\theta(1+j))} = \nabla_j \frac{\theta(1+j)(-1)^h}{(h+1)^{(r+\delta)/\delta}} \binom{\theta(1+j)-1}{h}$$

and $\Gamma(1+\delta)|_{(\delta \in R^+)} = \delta! \prod_{r=0}^{\delta-1} (\delta - r)$. where $E(y) = \mu'_{1,Y}$ is the mean of Y. The r^{th} incomplete moment, say $\phi_{r,Y}(t)$, of Y can be expressed, from (9), as

$$\phi_{r,Y}(t) = \int_{-\infty}^{t} y^r f(y) dy = \sum_{j=0}^{\infty} \nabla_j \int_{-\infty}^{t} y^r \pi_{\theta^\bullet}(y) dy$$

then

$$\phi_{r,Y}(t)|_{(r>-\delta)} = b^r \gamma\left(r\delta^{-1} + 1, t^\delta\right) \sum_{j,h=0}^{\infty} \nabla_{j,h}^{(r,\theta(1+j))},$$

where $\gamma(\delta, r)$ refers to the incomplete gamma function where

$$\gamma(\delta, r)|_{(\delta \neq 0,-1,-2,\ldots)} = \int_0^r y^{\delta-1} exp(-y)\, dy = \frac{1}{\delta} r^\delta \{F_{1,1}[\delta; \delta+1; -r]\} = \sum_{j=0}^{\infty} \frac{(-1)^j}{j!(\delta+j)} r^{\delta+j},$$

and $F_{1,1}[\cdot,\cdot,\cdot]$ is a confluent hypergeometric function. The first incomplete moment can be derived from (10) with $r = 1$ as

$$\phi_{1,Y}(t)|_{(1>-\delta)} = b\gamma\left(\delta^{-1} + 1, t^\delta\right) \sum_{j,h=0}^{\infty} \nabla_{j,h}^{(1,\theta(1+j))}.$$

3.3 Moment generating function (MGF)

The MGF $M_y(t) = E(exp(tY))$ of Y can be derived from equation (8) as $M_Y(t) = \sum_{j=0}^{\infty} \nabla_j M_{\theta\bullet}(t)$ where $M_{\theta\bullet}(t)$ is the MGF of the F model with scale parameter $\theta^{\bullet\frac{1}{\theta}}$ and shape parameter θ, then

$$M_Y(t)|_{(r>-\delta)} = \sum_{r=0}^{\infty}\sum_{j,h=0}^{\infty} \frac{t^r}{r!} b^r \Gamma(1 + r\delta^{-1}) \nabla_{j,h}^{(r,\theta(1+j))}.$$

3.4 Numerical analysis

Numerical analysis of mean (E(Y)), variance (V (Y)), skewness (S (Y)), kurtosis (K (Y)) and dispersion index (DisIx (Y)) for probability distributions is important for several reasons:

I. Descriptive statistics: Mean, variance, skewness, kurtosis, and dispersion index are descriptive statistics that provide valuable insights into the shape and characteristics of probability distributions. They summarize the central tendency, spread, symmetry, and tail behavior of the distributions, allowing for a concise and quantitative description of the data.

II. Comparison of distributions: By analyzing these numerical measures, one can compare different probability distributions and understand how they differ in terms of central tendency, variability, and shape. This is particularly useful when choosing the most appropriate distribution for modeling or when comparing different models.

III. Model selection and fitting: When fitting probability distributions to data, numerical analysis of these statistical measures helps in the selection of the best-fitting distribution. For example, comparing the sample mean and variance with the theoretical values of the mean and variance of a candidate distribution can indicate how well the distribution fits the data.

IV. Identification of departures from assumptions: Probability distributions often come with certain assumptions about their shape, symmetry, and tail behavior. Analyzing the skewness and kurtosis of the data relative to the theoretical values of the distribution can reveal departures from these assumptions. This is important for assessing the validity of using a particular distribution and identifying cases where alternative models or modifications may be more appropriate.

V. Risk assessment and decision-making: Measures such as skewness and kurtosis provide insights into the tail behavior and risk characteristics of the distribution. Skewness indicates the asymmetry of the distribution, while kurtosis measures the degree of heavy tails or outliers. These measures are valuable in risk assessment, financial modeling, and decision-making, where understanding extreme events and tail risk is critical.

VI. Data quality assessment: Numerical analysis of mean, variance, and other statistical measures can be used to evaluate the quality and consistency of the data. Extreme values or inconsistencies in these measures may indicate data errors, outliers, or anomalies that need to be investigated further.

VII. Interpretation and communication: Mean, variance, skewness, kurtosis, and dispersion index provide interpretable and quantifiable measures that can be easily communicated to stakeholders or decision-makers. They summarize key characteristics of probability distributions in a way that is accessible and meaningful to a broad audience.

Table 1 gives numerical calculations and analysis for the **E**(Y), **V** (Y), **S** (Y), (**K** (Y) and DisIx (Y). Based on results of Table 1, we note that:

I. The skewness of the OB-EW model can be positive and negative.

II. The spread for the OB-EW kurtosis is much larger ranging from 2.77 to ∞

III. DisIx(Y) can be "between 0 and 1" or "more than 1".

Table1: numerical analysis for some measures.

a	b	θ	δ	**E**(Y)	**V**(Y)	**S**(Y)	**K**(Y)	DisIx(Y)
1	1.5	1.5	1.5	0.8800320	0.2334306	0.8736123	3.953436	0.26525230
5				0.9545571	0.0135419	−0.0481334	3.734373	0.01418659
10				0.9740506	0.0035521	−0.2170822	3.931679	0.00364678
15				0.9811216	0.0016025	−0.2729389	4.013721	0.00163338
20				0.9847622	0.0009079	−0.3004402	4.056618	0.00092201
25				0.9869797	0.0005836	−0.3167544	4.082711	0.00059126
35				1.823×10^{-6}	1.497×10^{-6}	671.7073	451199.1	0.82195150
45				1.811×10^{-8}	1.488×10^{-8}	6737.699	45396625	0.82193460
50				1.769×10^{-9}	1.454×10^{-9}	21556.76	46469401	0.82193380
3	1	2.5	1.75	1.228339	0.03323537	0.3401759	4.000098	0.02705717
	5			1.02498	0.01399285	−0.4985881	3.501640	0.01365183
	10			0.9590106	0.01159832	−0.5882747	3.552380	0.01209405
	20			0.8990309	0.00992206	−0.6249063	3.575097	0.01103639
	50			0.8265806	0.00822149	−0.6396704	3.580426	0.00994639
	100			0.776122	0.00716234	−0.6413326	3.578822	0.00922837
	200			0.7290233	0.00624309	−0.6408311	3.578074	0.00856364
	500			0.671523	0.00520430	−0.6404336	3.581039	0.00774999
5	5	0.1	3	0.05120718	0.00056081	−13.299380	70.19642	0.01095171
		0.25		0.2973598	0.00376104	−0.3829631	3.211746	0.01264813
		0.5		0.5574816	0.00417322	−0.6861096	3.922469	0.00748584
		5		1.2125185	0.00131563	−0.7891039	4.321758	0.00108504
3.5	10	3.5	0.001	0.0198901	0.2991525	36.554780	1503.942	15.04029
			0.1	7.865513	69.071410	0.9380262	2.770844	8.781551
			0.5	1.634906	0.1883477	−0.0327175	2.859176	0.115204
			2.5	1.096388	0.0039961	−0.7720786	4.068018	0.003645
			5	1.046638	0.0009356	−0.8882429	4.457864	0.000894
			20	1.02×10^{-18}	8.42×10^{-19}	$\cong\infty$	$\cong\infty$	0.821934
1	1	1	1	1	1	2	9	1
1	1	1	2	0.8862269	0.2146018	0.6311107	3.245089	0.2421522
10	10	1	2	0.7499304	0.00139751	−0.9115916	4.587999	0.00186352
1	1	10	20	1.79×10^{-14}	2.13×10^{-19}	8178952	$\cong\infty$	1.18987
0.05	0.05	0.05	0.05	0.00275907	0.04211283	98.0229	10779.11	15.26341

3.5 Entropies

The Rényi entropy offers a versatile framework for quantifying uncertainty, complexity, and information in various contexts. Its different forms allow for customized analyses based on the specific requirements of the problem at hand, making it a valuable tool in statistical theory and a wide range of applications. The Rényi entropy of a random variable Y represents a measure of variation of the uncertainty defined by

$$R_{\nabla}(Y)=\frac{1}{1-\nabla}log\left[\int_{-\infty}^{\infty}f(y)^{\nabla}dy\right]|_{\nabla>0 \text{ and } \nabla\neq 1}.$$

Based on the PDF (6) and following similar algebra of Subsection 2.1, we can write

$$f(x)^{\nabla}=\sum_{j,k=0}^{\infty}\sum_{i=0}^{k}E_{i,j,k}(\nabla)\ h_{\theta,\delta}(y;\nabla)H_{\theta,\delta}(y;j+\alpha(k+\nabla-i)-\nabla)|_{j+k\geq 1},$$

where

$$h_{\theta,\delta}(y;\nabla) = \left[h_{\theta,\delta}(y)\right]^{\nabla}, H_{\theta,\delta}(y;\alpha(k-i+\nabla)+j-\nabla)\left[H_{\theta,\delta}(y)\right]^{\alpha(k-i+\nabla)+j-\nabla}$$

and

$$E_{i,j,k}(\nabla) = a^{\nabla}b^{\nabla}\frac{(-1)^{i}\Gamma(a(k-i+\nabla)+\nabla+j)}{2^{\nabla(b+1)+k}j!\,\Gamma(a(k-i+\nabla)+\nabla)}\binom{k}{i}\binom{-\nabla(b+1)}{k}.$$

Then, the Rényi entropy of Y is given by

$$R_{\nabla}(Y) = \frac{1}{1-\nabla}\log\left[\sum_{j,k=0}^{\infty}\sum_{i=0}^{k}E_{i,j,k}(\nabla)\,\mathbf{I}_0^{\infty}(Y;\nabla)\right], \tag{11}$$

where

$$\mathbf{I}_0^{\infty}(Y;\nabla) = \int_0^{\infty} h_{\theta,\delta}(y)^{\nabla}\,H_{\theta,\delta}(y)^{\alpha(k-i+\nabla)+j-\nabla}dy.$$

The integral $\mathbf{I}_0^{\infty}(Y;\nabla)$ can be computed numerically for most baseline models. The Rényi entropy has applications in statistical theory and various fields, including:

I. Rényi entropy generalizes Shannon entropy and provides alternative measures of information and uncertainty. It is used in information theory to study data compression, coding theory, and data transmission.

II. Rényi entropy has applications in statistical estimation, hypothesis testing, and model selection. It can be used as a measure of goodness-of-fit between observed data and a proposed probability distribution. It also plays a role in information criteria, such as the Akaike Information Criterion (AIC) and the Bayesian Information Criterion (BIC).

III. Rényi entropy can be used to analyze and compare the complexity, diversity, or heterogeneity of data sets. It has applications in clustering, pattern recognition, feature selection, and data mining. Different values of α allow for emphasizing different aspects of the data distribution.

IV. Rényi entropy is employed in image and signal processing tasks, such as image segmentation, texture analysis, and image compression. It provides a measure of image complexity or texture irregularity, enabling the quantification and characterization of visual or signal information.

V. Rényi entropy is utilized in the study of complex systems, including physics, biology, and social sciences. It can capture the degree of disorder, phase transitions, and critical phenomena in these systems. Rényi entropy is applied in the field of quantum information theory to analyze entanglement and quantum complexity.

Equation (11) can be evaluated numerically for different parameters value and then can plotted for exploring the Rényi entropy index. Figure 3 gives some plots for the Rényi entropy index for different parameters value where for $a = 0.5, b = 10, \theta = 1, \delta = 1$ see Figure 3 (top left panel), for $a = 0.5, b = 10, \theta = 3, \delta = 1$ see Figure 3 (top middle panel), for $a = 0.5, b = 10, \theta = 3.85, \delta = 1$ see Figure 3 top right panel), for $a = 0.5, b = 10, \theta = 5, \delta = 1$ see Figure 3 (middle left panel) for $a = 0.5, b = 10, \theta = 5, \delta = 0.4$ see Figure (3 middle middle panel), for $a = 0.5, b = 10, \theta = 5, \delta = 10$ see Figure (3 middle right, for $a = 0.5, b = 10, \theta = 5, \delta = 20$ see Figure (3 bottom left panel), for $a = 0.25, b = 15, \theta = 5, \delta = 1$ see Figure (3 bottom middle panel), for $a = 0.15, b = 15, \theta = 5, \delta = 1$ see Figure (3 bottom right panel) Based on Figure 3, it is noted that the Rényi entropy can have many useful shapes. The Shannon entropy of a random variable Y, say SE, is special case of the Rényi entropy when $\nabla \uparrow 1$. Then, the SE can be expressed as $E[-log\, f\,(Y)]$.

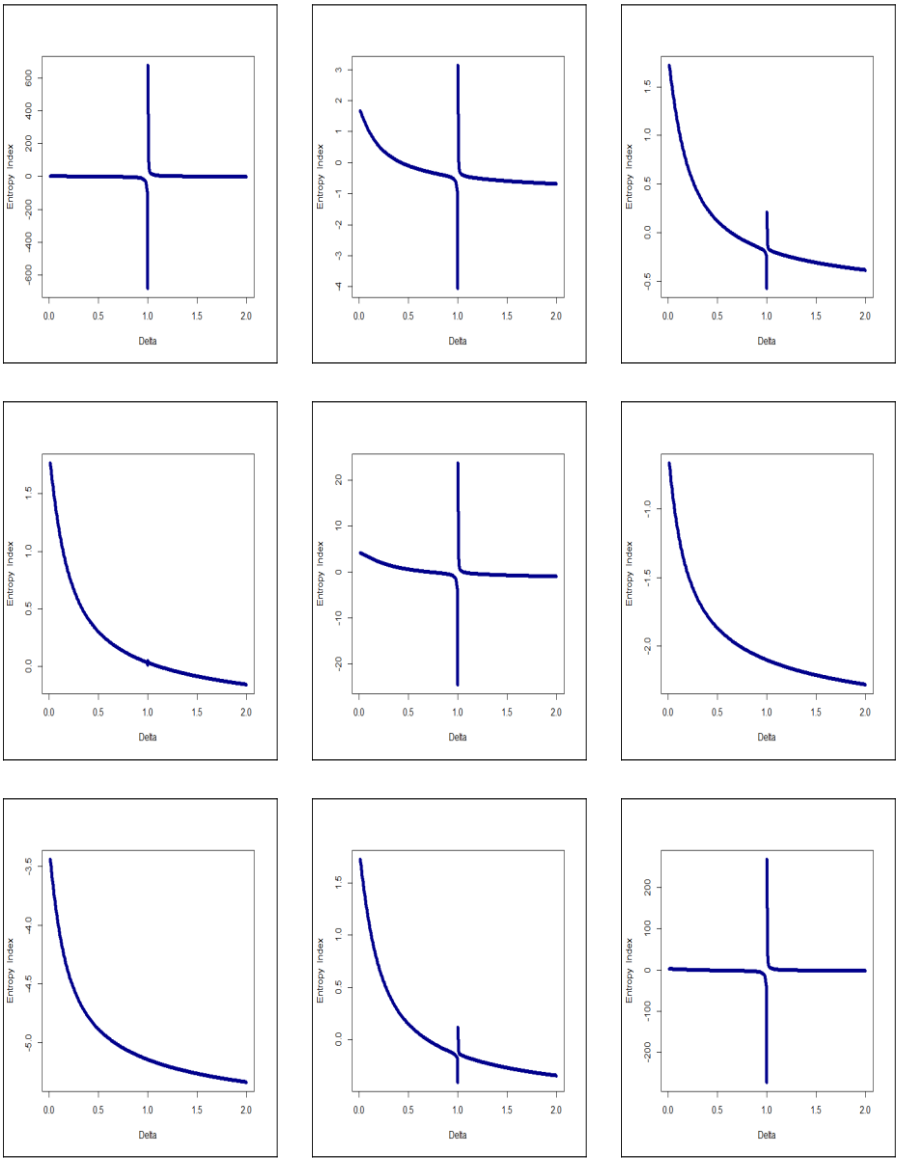

Figure 3: Rényi entropy index.

4.Graphical assessment

Graphical simulation studies in the theory of probability distributions offer several advantages, providing visual representations of distributions and aiding in the analysis and understanding of their properties. Here are the key advantages of graphical simulation studies:

I. Graphical simulations provide visual representations of probability distributions, making complex mathematical concepts more accessible and easier to understand. By visually depicting the distribution's shape, density, and characteristics, graphical simulations offer an intuitive and immediate grasp of the distribution's behavior.

II. Graphical simulations help researchers and practitioners gain insights into the properties of probability distributions. Visualizations such as probability density functions (PDFs), cumulative distribution functions (CDFs), and quantile-quantile (Q-Q) plots allow for the examination of characteristics like skewness, kurtosis, tail behavior, and mode. These insights can inform decision-making, model selection, and further analysis.

III. Graphical simulations enable the comparison of different probability distributions side by side. Overlaying multiple PDFs or CDFs on the same plot facilitates visual comparisons of their shapes, location, spread, and tail behavior. This aids in the selection of the most appropriate distribution for a given dataset or problem, helping to identify the best-fitting distribution.

IV. By visually examining the effects of parameter changes on the shape of a distribution, graphical simulations facilitate sensitivity analysis. Researchers can manipulate distribution parameters, such as mean, variance, or shape parameters, to observe the resulting changes in the distribution's characteristics. This allows for a deeper understanding of how variations in parameters impact the distribution.

V. Graphical simulations provide concrete illustrations of theoretical concepts related to probability distributions. For example, they can demonstrate how changing parameters affect the location, spread, and shape of a distribution. This visual representation aids in teaching and learning about probability distributions and associated concepts.

VI. Graphical simulations offer an effective means of communicating and presenting distribution-related findings. Visual representations allow for clear and concise communication of complex concepts to a wide range of audiences. The use of graphs, histograms, or other visualizations can enhance the clarity and impact of research or analysis outcomes.

VII. Graphical simulations can help identify outliers and unusual observations in datasets. By comparing the observed data to the expected distribution, researchers can visually spot deviations and anomalies, which may indicate data quality issues, errors, or the presence of rare events.

The implementation of graphical simulation studies has the potential to make important contributions to the development of the field of probability distributions study in a number of different and significant ways. They make it feasible to do sensitivity studies, compare and select different distributions, compare and demonstrate theoretical concepts, aid in communication and presentation, and provide assistance in identifying outliers. In addition to this, they provide graphics that are easy to use, offer insights into the features of distributions, and make it much simpler to evaluate and choose between different distributions. These benefits lead to a more in-depth understanding of probability distributions, as well as their application in the real life across a wide range of business sectors. In addition, this understanding contributes to the development of new business opportunities. We are able to carry out the simulation experiments in order to evaluate the finite sample behavior of the MLEs by doing so graphically and by making use of the mean squared errors (MSEs) in addition to the biases. This allows us to analyze the behavior of the MLEs over a finite number of samples. This enables us to conduct an analysis of the MLEs' behavior across a set number of samples. During the performance of the evaluation, the following methods were applied as part of the process:

I. Generate $N = 1000$ samples of size $n|_{(n=50,100,\ldots,1000)}$ from the OB-EW distribution using (7);

II. Compute the MLEs for the $N = 1000$ samples;

III. Compute the SEs of the MLEs for the 1000 samples;

IV. The standard errors (SEs) were computed by inverting the observed information matrix;

V. Compute the biases and mean squared errors given for $\underline{V} = a, b, \alpha, \beta$. We repeated these steps for $n|_{(n=50,100,\ldots,750)}$ with $a = b = \theta = \delta = 1$, so computing biases $\left(\text{Bias}_{\underline{P}}(n)\right)$, mean squared errors $(MSE_h(n))$ for $\underline{V} = a, b, \theta, \delta$ and $n|_{(n=50,100,\ldots,1000)}$.

The mean square errors, which are also referred to as MSEs, are displayed in the panels located on the right side of figures 3, 4, 5, and 6. The biases are displayed in the panels located on the left side of the same figures. The panels on the left describe how all biases move as the value of n is increased or decreased by illustrating this shift in relation to each other. This shift is shown in the context of the other shifts. The right panels show how the four MSEs respond to different values of n based on how the computations for each of them are carried out. These values are shown in the panel on the right. After the line is broken, as seen in Figure 4, the biases are deemed to be at their utmost level of accuracy. The graph gives clear evidence of this point. The data presented in the figure makes this point quite evident. On the basis of Figures 3-6, it is possible to establish that the MSEs for each parameter move closer to zero as n gets smaller, and that the biases for each parameter regularly have negative values and grow closer to zero as n gets smaller. Additionally, it is possible to demonstrate that the biases for each parameter frequently have negative values, and that this trend continues as n gets smaller. It is possible to demonstrate, by this method, that the biases and MSEs for each parameter are connected to one another. The fact that the mean squared errors for each parameter likewise go closer and closer to zero as n gets smaller as the number of observations in the research gets down lends credence to the findings that can be supported by this observation.

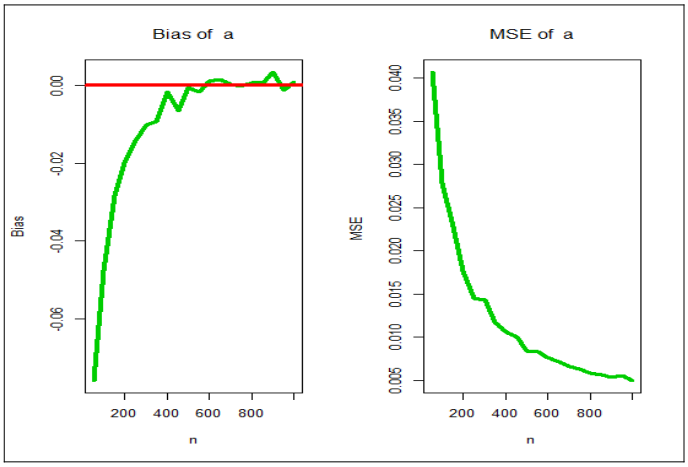

Figure 4: Biases (left) and mean squared errors (right) for the parameter a.

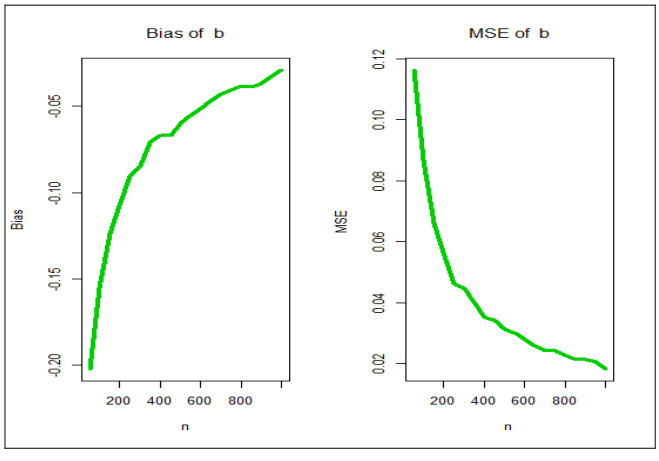

Figure 5: Biases (left) and mean squared errors (right) for the parameter b.

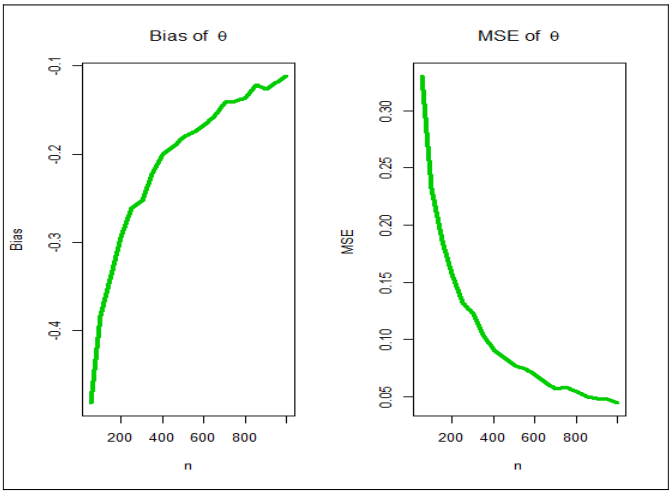

Figure 6: Biases (left) and mean squared errors (right) for the parameter θ.

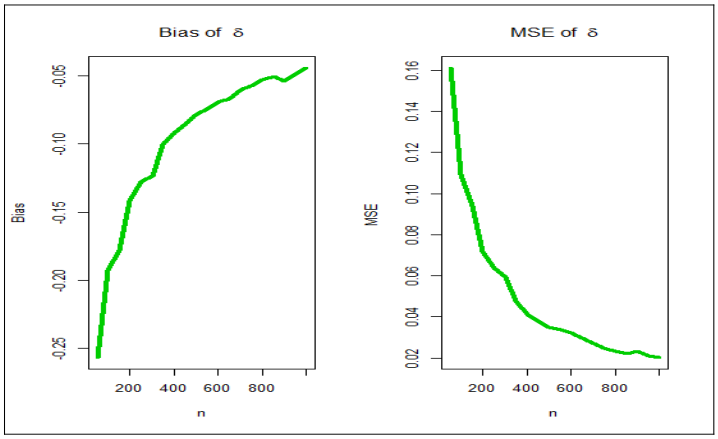

Figure 7: Biases (left) and mean squared errors (right) for the parameter δ.

5. Applications

Real data modeling plays a crucial role in illustrating the flexibility of probability distributions. Here are some reasons why it is important:

I. Real data modeling allows us to choose the most suitable probability distribution to represent a given dataset. By analyzing the characteristics of the data and considering its distributional properties, we can select a distribution that accurately captures the patterns and variations present in the data. This ensures that our modeling efforts reflect the true nature of the data and lead to meaningful insights.

II. Real data modeling enables us to test hypotheses about the underlying distribution of a dataset. By fitting different distributions to the data and comparing their goodness-of-fit, we can evaluate the plausibility of different distributional assumptions. This process helps us validate or reject specific hypotheses and provides evidence for the appropriateness of a chosen distribution.

III. Real data modeling allows us to estimate the parameters of probability distributions from observed data. By fitting a distribution to the data, we can estimate the values of its parameters, which provide valuable information about the distribution's characteristics. These estimated parameters can then be used for inference, prediction, and decision-making purposes.

IV. Real data modeling with probability distributions enables us to make predictions and forecasts. Once we have identified an appropriate distribution for the data, we can utilize it to generate probabilistic forecasts of future outcomes. This helps in understanding the uncertainty associated with predictions and aids in

decision making under uncertain conditions.

V. Real data modeling allows us to simulate data based on chosen probability distributions. By generating synthetic data that follows a specific distribution, we can create scenarios for risk analysis and evaluate the potential outcomes of different situations. This helps in assessing and managing risks by understanding the range of possible outcomes and their probabilities.

VI. Real data modeling allows us to assess the sensitivity of results to changes in the underlying distribution. By considering alternative distributions or variations in distributional parameters, we can examine how sensitive our results are to different modeling assumptions. This analysis helps in understanding the robustness of conclusions and decision-making processes.

In a nutshell, it is not possible to demonstrate the flexibility of probability distributions without making use of real data modeling. It is helpful in precisely describing data, testing hypotheses, estimating parameters, making forecasts, running simulations, evaluating risks, and determining how sensitive results are to changes. Additionally, it can execute simulations. We are able to demonstrate the adaptability of probability distributions as well as the huge variety of fields in which probability distributions may be applied because we use real data in the process of modeling. This is made possible by the use of actual data.

Application I

These are the failure times for each of the 84 observations that make up the data, as indicated by the findings that Murthy et al. (2004) came to the conclusion about, see Yousof et al. (2017a) and Korkmaz (2018a,b) for details. Figure 8(a) provides a visual representation of the total time test (TTT) plot for the initial data. This plot was developed with the assistance of Aarset (1987). It is possible to demonstrate, using this plot as evidence, that the empirical HRF of the first data is "monotonically increasing." Box plots and Quantile-Quantile plots, also known as Q-Q plots, are depicted, respectively, in Figures 7(b) and 7(c), which are mirror images of one another. Figure 7 presents both of these graphs for your perusal. At least according to Figures 7(b) and 7(c), it would appear that this data set does not contain any outliers. This conclusion is based on the data. The nonparametric Kernel density estimate (NKDE) is shown in Figure 8(d). This is an analytical technique that can be used in order to investigate the data form and may be seen as a representation of the figure. After examining Figure 8(d), we have determined that the data on the failure times have a distribution that is both bimodal and semisymmetric. This was discovered as a result of our examination of the aforementioned figure. In this section, we will evaluate the OB-EW distribution in comparison to other competing models by analyzing how well it fits the data. The Marshall Olkin extended-W (MO-EW), the beta-W (B-W), the Transmuted Modified-W (TM-W), the modified beta-W (MB-W), and the transmuted exponentiated generalized-W (TEG-W) are some of the other models that are included in this category. Table 2 displays the mean linear estimates (MLEs) along with the standard errors (SEs) that correspond to them for each of the competing models. Table 3 provides the values for the CVM (Cramér–von Mises) and AD (Anderson–Darling) statistics for each of the competing models. In addition to its more common name, the CVM statistic is also known as the Anderson–Darling statistic. The Cramér–von Mises statistic is what is meant to be represented by the abbreviation CVM. According to Table 3, the OB-EW model produces the lowest values of the statistics that were used (CVM = 0.3879 and AD =2.3574) and, as a result, offers the best fit to the first data sets. This is because the model generates the lowest values of the statistics that were utilized. The estimated PDF (ECDF), estimated CDF (ECDF), estimated HRF (EHRF), and probability versus probability (P-P) graphs for the first set of data are depicted in figure 9. When one looks at Figure 9, it becomes instantly clear that the OB-EW model that was presented offers fits that are acceptable to the empirical function. This becomes immediately evident when one looks at the figure.

Table 2: MLEs (standard errors (SEs)) for the 1st data set.

Distribution			Estimates (SEs)	
MOEW(a,θ,δ)	488.8992	0.28321	1261.975	
	(189.358)	(0.0134)	(351.072)	
OB-EW(a,b,θ,δ)	**0.13479**	**0.66701**	**0.03533**	**2.27098**
	(0.0342)	**(0.2031)**	**(0.002)**	**(0.0023)**
Beta-W(a,b,θ,δ)	1.36433	0.29812	34.1802	11.4956
	(1.0023)	(0.0632)	(14.838)	(6.7233)
TrMW(a,b,θ,δ)	0.27221	1.00019	4.6×10^{-6}	0.46854

	(0:0143)	(5.2×10^{-5})	(1.9×10^{-4})	(0.1656)	
MBW$(a, b, c, \theta, \delta)$	10.1502	0.16325	57.4167	19.3858	2.00413
	(18.6917)	(0.0195)	(14.063)	(10.019)	(0.6624)
TrEGW$(a, b, c, \theta, \delta)$	4.25637	0.15332	0.0978	5.23133	1173.31
	(33.4012)	(0.0174)	(0.609)	(9.7924)	(6.9998)

Table 3: CVM and AD for the 1st data set.

Distribution	CVM	AD
OB-EW	**0.38791**	**2.35742**
MO-EW	0.39953	4.44771
Beta-W	0.46524	3.21972
TrMW	0.80658	11.2047
MBW	0.47179	3.26568
TrEGW	1.00792	6.23323

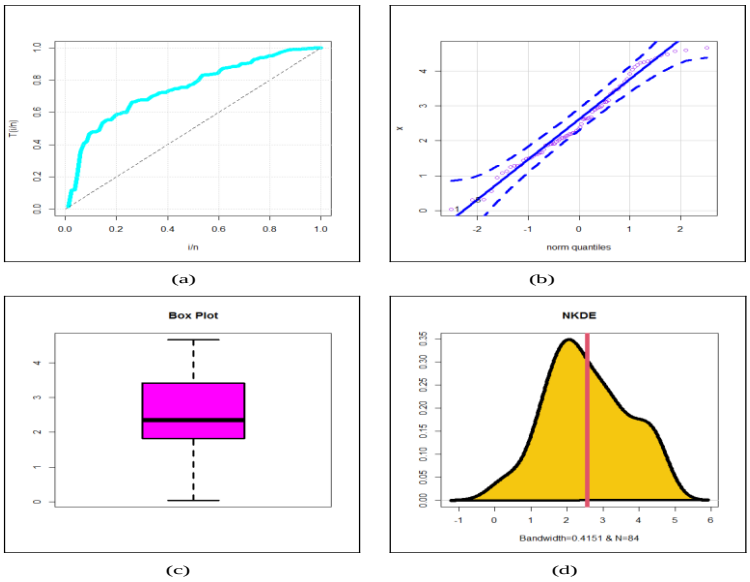

Figure 8: TTT plot(a), Q-Q plot(b), box plot(c) and NKDE(d) for the 1st data.

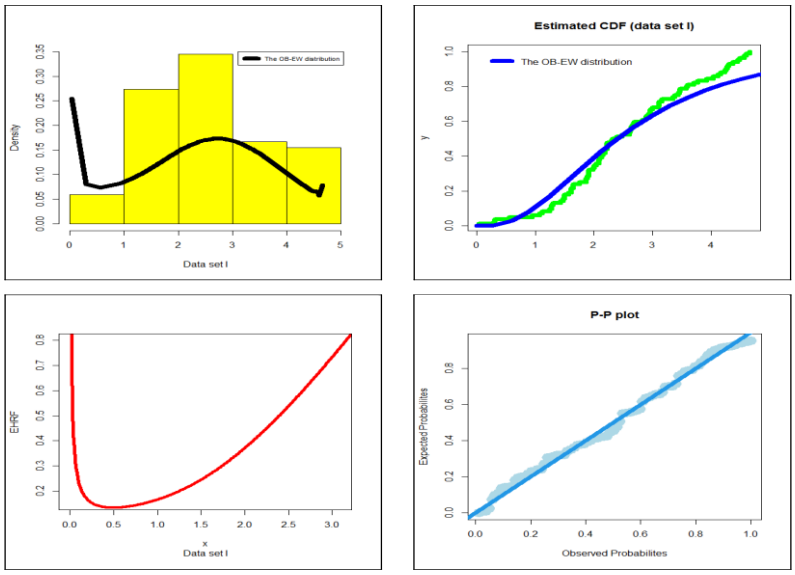

Figure 9: EPDF, ECDF, EHRF and P-P plot for the 1st data.

Application II

The survival times (in days) of 72 guinea pigs that Bjerkedal (1960) reported were infected with virulent tubercle bacilli is the subject of the third real data set. Figure 10(a) displays the TTT plot that was generated using the second set of data. This observation offers support for the hypothesis that the empirical HRF of the second data set is "monotonically increasing." Box plots and Q-Q plots, which are depicted similarly in figures 9(b) and 9(c), respectively, are demonstrated to coincide with one another. On the basis of the data shown in Figures 9b and 7c, it is possible to single out a few instances of extreme behavior. The NKDE, which can be applied in order to explore the shape of the data, is depicted in Figure 10(d). Figure 10d reveals that the data for survival times has a bimodal distribution and is right skewed, as expected given the nature of the data. It is clear from looking at the data that are shown in Figures 11b and 11c that there are a few outliers in the data. In comparison to the OB-EW distribution, we are going to test the Odd Weibull-Weibull (OW-W), gamma exponentiated-exponential (GaEE), and EW distributions to determine how well they fit our data. The MLEs and SEs for each of the competing models are listed in Table 4, along with their corresponding MLEs and SEs. The values for the C-V-M and A-D statistics for all of the competitive models that were taken into consideration are presented in Table 5. According to Table 5, the OB-EW model is the one that offers the best fit to the 2nd data sets since it yields the lowest values for the statistics that were used ((CVM= 0.0767 and AD=0.4941)). Figure 11 displays the EPDF, ECDF, EHRF, and P-P plots that were generated from the second set of data. As can be seen in Figure 11, the OB-EW model appears to produce fittings to the empirical function that are satisfactory.

Table 4: MLEs (SEs) for the 2nd data set.

Distribution	Estimates (SEs)		
BX(θ, δ)	0.93658.3	0.004783	
	(0.14612)	(0.00049)	
TrBX(a, θ, δ)	0.632772	1.039173	0.004171
	(0.24514)	(0.14435)	(0.00053)
OLEW(a, θ, δ)	0.00183	0.07164	0.281332
	(0.00049)	(0.02543)	(0.00909)

OW-W(a,θ,δ)	11.15761	0.08816	0.457346	
	(4.5449)	(0.0365)	(0.08216)	
GaE-E(a,θ,δ)	2.11388	2.60036	0.00834	
	(1.32885)	(0.55979)	(0.0059)	
OB-EW (a,b,θ,δ)	**0.33533**	**0.15611**	**1.12901**	**0.5700**
	(0.07912)	**(0.0392)**	**(0.02612)**	**(0.0021)**

Table 5: CVM and AD for the 2nd data set.

Distribution	CVM	AD
OB-EW	0.07671	0.494131
BX	0.18499	1.085781
TrBX	0.13526	0.792592
OLEW	0.25177	1.47532
OW-W	0.44945	2.476401
GaE-E	0.3157	1.720802

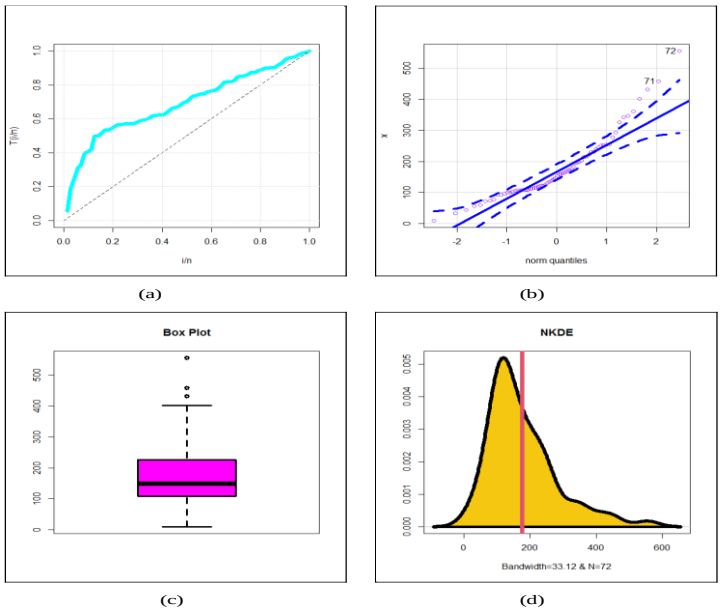

Figure 10: TTT plot(a), Q-Q plot(b), box plot(c) and NKDE(d) for the 2nd data.

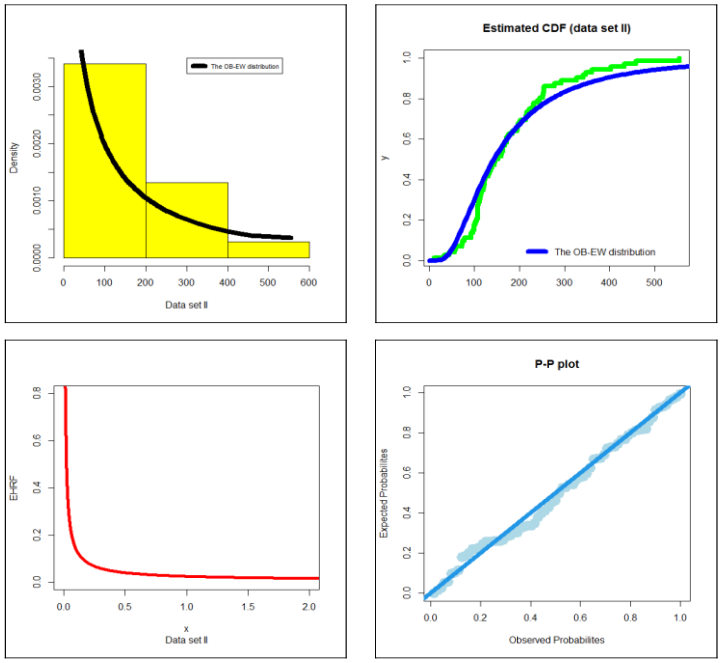

Figure 11: the EPDF, ECDF, EHRF and P-P plot for the 2nd data.

Application III

These 63 measurements of the strengths of glass fibers measuring 1.5 centimeters in length were initially acquired by employees working at the United Kingdom National Physical Laboratory (for additional information, see Smith and Naylor (1987)). The TTT plot for the third data is depicted in Figure 12a. This plot illustrates that the empirical HRF of the third data is "monotonically increasing." Taking a look at the figure makes this quite clear. It has been established that box plots and Q-Q plots, which are depicted identically in figures 11(b) and 11(c), respectively, coincide with one another. Exploring the data shape can be accomplished with the assistance of the NKDE, as shown in Figure 12(d), which can be found here. According to Figure 12(d), the data on the strengths have a bimodal distribution, and they are skewed to the left. This is the case despite the fact that they are biased to the left. The figure illustrates this point quite clearly. In the case of the third data set, we will evaluate the degree to which the OB-EW distribution fits the data in comparison to the degree to which other distributions, such as the EW, T-W, and OLL-W distributions, match the data. To be more specific, we will evaluate the degree to which the OB-EW distribution fits the data in comparison to the degree to which other distributions match the data. In Table 6, you will find a listing of both the MLEs and SEs for each of the competing models, as well as the MLEs and SEs that correlate to them. Table 7 contains the data for the C-V-M and A-D statistics for each of the various competing models that were investigated. According to Table 7, the OB-EW model provides the best fit to the 3rd data sets since it yields the lowest values for the statistics that were utilized (CVM=0.2259 AD=1.2296) In addition, this model provides the best fit to the 2nd data sets as well. This is the case since the values that this model produces for the statistics that were used are the lowest of any other model. Figure 13 depicts the EPDF plot, together with the ECDF plot, the EHRF plot, and the P-P plot for the third data set. Additionally, the EHRF plot is shown. Figure 13 demonstrates that the fits produced by the OB-EW model to the empirical function appear to be good. This may be seen in the figure.

Table 6: MLEs (SEs) for the 3rd data set.

Distribution	Estimates (SEs)		
BX(θ, δ)	5.48597	0.98682	
	(1.1853)	(0.0540)	
TrBX(a, θ, δ)	-0.65524	4.78605	1.04504

	(0.19529)	(1.2831)	(0.0549)	
OLBX(a,θ,δ)	0.658314	2.10191	0.8429	
	(0.5112)	(1.2446)	(0.0548)	
OLEW(a,θ,δ)	0.50878	2.53424	1.71224	
	(0.39744)	(1.8298)	(0.0959)	
EW(a,θ,δ)	0.67122	7.2855	1.7148	
	(0.24943)	(1.707)	(0.0865)	
TrW(a,θ,δ)	-0.50101	5.14981	0.6458	
	(0.27411)	(0.6657)	(0.0235)	
OLLW(a,θ,δ)	0.94329	6.02564	0.61595	
	(0.2689)	(1.3478)	(0.0164)	
OB-EW(a,b,θ,δ)	0.57872	0.22520	2.06691	4.45479
	(0.16311)	(0.0733)	(0.8581)	(0.0025)

Table 7: CVM and AD for the 3rd data set.

Distribution	CVM	AD
OB-EW	0.22592	1.22966
OLBX	0.25572	1.41542
TrBX	0.47641	2.61632
OLEW	0.27111	1.49653
BX	0.55194	3.07222
EW	0.63631	3.48428
TrW	1.03508	0.16917
OLLW	1.23644	0.21944

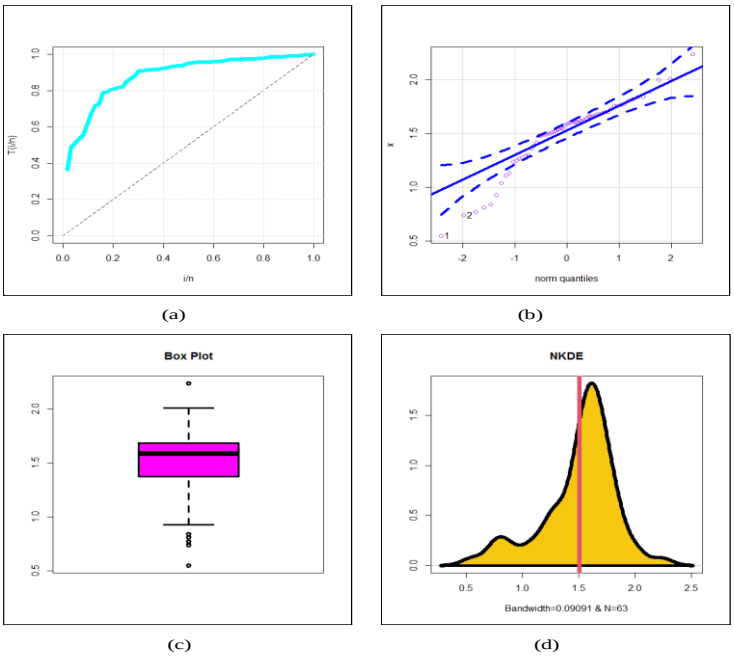

Figure 12: TTT plot(a), Q-Q plot(b), box plot(c) and NKDE(d) for the 3rd data.

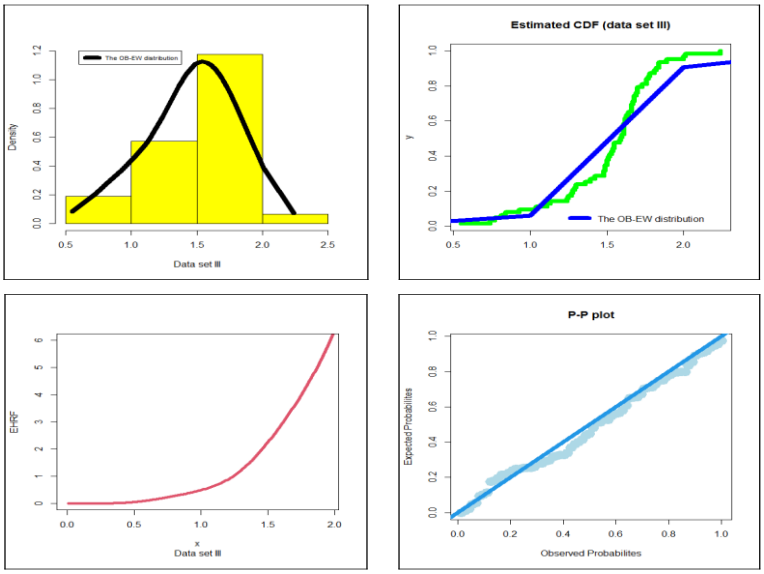

Figure 13: the EPDF, ECDF, EHRF and P-P plot the 3rd data.

6. Concluding remarks

The writers of this work explain a novel variation of the exponentiated Weibull distribution that they have designed themselves and that is detailed in this research study. The research study itself is referred to in the authors' discussion. The folks who were in charge of writing the study are the ones who are referred to as the authors of this work. After the appropriate mathematical properties have been derived, it is necessary to conduct out an analysis of those properties in order to fully understand them. In addition to the variance, skewness, and kurtosis, the dispersion index, and the incomplete moment, a numerical assessment of the value that was predicted is carried out. The increased density can be represented by a variety of different helpful shapes, including "bathtub," "bimodal and left skewed," "right skewed," "bimodal and right skewed," and "unimodal and left skewed," in addition to "bathtub." These forms can be found in the table below. The table that follows contains these forms for your convenience. The following table gives an overview of all of these different kinds of forms. The new rate of failure could alternatively be referred to as "bathtub (U-HRF)", "constant", "monotonically increasing", "upside down-increasing (reversed U-increasing)", "J-HRF", "upside down-constant", " monotonically decreasing", "increasing-constant", or "upside down (reversed U)". Graphical analysis is a helpful tool that may be utilized in the process of determining whether or not the strategy of maximum likelihood is successful. The biases and the mean squared errors are the major metrics that should be utilized for evaluation purposes within the framework of this approach. A scenario is presented to the reader that graphically demonstrates the adaptability and utility of the creative distribution. This is achieved by utilizing three different sets of actual data at the same time. As a future points, one may allocate some efforts for studying the following points:

- **I.** Risk analysis and estimation under the OB-EW model (see Khedr et a;. (2023), Emam et al. (2023a,b), Ibrahim (2023) and Yousof (2023a,b,c) for more details and applications).
- **II.** Quality control testing under the OB-EW model (see Aryal et al. (2017) and Tashkandy et al. (2023) for more details and applications).
- **III.** Distributional validations under the OB-EW model (see Goual and Yousof (2020), Mansour et al. (2020c,d,e,f), Tashkandy et al. (2023), Ibrahim (2019 and 2022) Yadav et al. (2022) and Khalil et al. (2023) for more details and applications)

Here are some other future research points:

- **I.** Investigate how the novel OB-EW distribution interacts with various copula functions to model complex dependence structures. Explore how the copula approach can enhance the flexibility of the distribution in capturing multivariate data (see Elgohari and Yousof (2021a,b,c) and Elgohari et al. (2021))

II. Compare and contrast different methods for estimating the parameters of the OB-EW distribution. Consider both classical methods and modern computational techniques, highlighting their strengths and limitations (see Shehata et al. (2021 and 2022)).

III. Develop and evaluate goodness-of-fit tests tailored specifically for the OB-EW model. Explore how well the distribution fits various types of data and assess its performance against other well-known distributions (see Ibrahim et al. (2021), Yousof et al. (2022) and Khalil et al. (2023)).

IV. Explore Bayesian methods for parameter estimation and model selection within the context of the OB-EW model. Discuss the advantages of Bayesian approaches and their applicability to real-life data.

V. Extend the OB-EW model to the multivariate setting. Investigate its properties, copula-based extensions, and applications in modeling joint distributions of related variables (see Elsayed and Yousof (2019, 2020 and 2021)).

VI. Develop statistical tests and inference procedures based on the OB-EW distribution. Consider applications in survival analysis, reliability, and other relevant domains (see Al-babtain et al. (2019)).

VII. Apply the new model to various real-life datasets, such as healthcare, finance, engineering, and environmental sciences. Demonstrate its effectiveness in capturing complex data patterns and making accurate predictions (see Shehata and Yousof (2021 and 2022)).

VIII. Conduct comprehensive comparative studies between the OB-EW distribution and existing distributions. Analyze their performance in terms of fit, prediction accuracy, and parameter interpretability (see Abouelmagd et al. (2019a.,b,c,d)).

IX. Develop user-friendly software packages or functions for fitting the OB-EW and conducting associated analyses. Consider integrating it with existing statistical software for wider accessibility.

X. Explore the robustness of the OB-EW model to outliers and model assumptions. Perform sensitivity analyses to assess the impact of different parameter values on the distribution's behavior (see Aboraya et al. (2022a,b)).

XI. Presenting some new group acceptance sampling plans based on percentiles for the OB-EW model. Ahmed and Yousof (2022), Ahmed et al. (2022a,b), Saber et al. (2022) and Tashkandy et al. (2023).

References

1. Aarset, M. V. (1987). How to identify a bathtub hazard rate. IEEE Transactions on Reliability, 36(1), 106-108.
2. Al-babtain, A. A., Elbatal, I. and Yousof, H. M. (2020a). A New Flexible Three-Parameter Model: Properties, Clayton Copula, and Modeling Real Data. Symmetry, 12(3), 440.
3. Al-Babtain, A. A., Elbatal, I. and Yousof, H. M. (2020b). A new three parameter Fréchet model with mathematical properties and applications. Journal of Taibah University for Science, 14(1), 265-278.
4. Aboraya, M., Ali, M. M., Yousof, H. M. and Ibrahim, M. (2022a). A New Flexible Probability Model: Theory, Estimation and Modeling Bimodal Left Skewed Data. Pakistan Journal of Statistics and Operation Research, 18(2), 437-463.
5. Aboraya, M., Ali, M. M., Yousof, H. M. and Ibrahim, M. (2022b). A Novel Lomax Extension with Statistical Properties, Copulas, Different Estimation Methods and Applications. Bulletin of the Malaysian Mathematical Sciences Society, 45, 85-120.
6. Abouelmagd, T. H. M., Hamed, M. S., Almamy, J. A., Ali, M. M., Yousof, H. M. and Korkmaz, M. C. (2019a). Extended Weibull log-logistic distribution. Journal of Nonlinear Sciences and Applications, 12(8), 523-534.
7. Abouelmagd, T. H. M., Hamed, M. S., Hamedani, G. G., Ali, M. M., Goual, H., Korkmaz, M. C. and Yousof, H. M. (2019b). The zero truncated Poisson Burr X family of distributions with properties, characterizations, applications, and validation test. Journal of Nonlinear Sciences and Applications, 12(5), 314-336.
8. Abouelmagd, T. H. M., Hamed, M. S., Handique, L., Goual, H., Ali, M. M., Yousof, H. M. and Korkmaz, M. C. (2019c). A new class of distributions based on the zero truncated Poisson distribution with properties and applications, Journal of Nonlinear Sciences & Applications (JNSA), 12(3), 152-164.
9. Abouelmagd, T. H. M., Hamed, M. S. and Yousof, H. M. (2019d). Poisson Burr X Weibull distribution. Journal of Nonlinear Sciences & Applications, 12(3), 173-183.

10. Ahmed, B. and Yousof, H. M. (2022). A New Group Acceptance Sampling Plans based on Percentiles for the Weibull Fréchet Model. Statistics, Optimization & Information Computing, forthcoming.
11. Ahmed, B., Ali, M. M. and Yousof, H. M. (2022a). A Novel G Family for Single Acceptance Sampling Plan with Application in Quality and Risk Decisions, Annals of Data Science, 10.1007/s40745-022-00451-3
12. Ahmed, B., Chesneau, C. Ali, M. M. and Yousof, H. M. (2022b). Amputated Life Testing for Weibull Reciprocal Weibull Percentiles: Single, Double and Multiple Group Sampling Inspection Plans with Applications, Pakistan Journal of Statistics and Operation Research, 18(4), 995-1013.
13. Bjerkedal, T., (1960). Acquisition of resistance in guinea pigs infected with different doses of virulent tubercle bacilli1. American Journal of Epidemiology. 72(1): p. 130-148.
14. Burr, I.W., (1942). Cumulative Frequency Functions. The Annals of Mathematical Statistics. 13(2): p. 215-232.
15. Elgohari, H. and Yousof, H. M. (2020a). A Generalization of Lomax Distribution with Properties, Copula and Real Data Applications. Pakistan Journal of Statistics and Operation Research, 16(4), 697-711.
16. Elgohari, H. and Yousof, H. M. (2021b). A New Extreme Value Model with Different Copula, Statistical Properties and Applications. Pakistan Journal of Statistics and Operation Research, 17(4), 1015-1035.
17. Elgohari, H. and Yousof, H. M. (2020c). New Extension of Weibull Distribution: Copula, Mathematical Properties and Data Modeling. Statistics, Optimization & Information Computing, 8(4), 972-993.
18. Elgohari, H., Ibrahim, M. and Yousof, H. M. (2021). A New Probability Distribution for Modeling Failure and Service Times: Properties, Copulas and Various Estimation Methods. Statistics, Optimization & Information Computing, 8(3), 555-586.
19. Elsayed, H. A. and Yousof, H. M. (2019). A new Lomax distribution for modeling survival times and taxes revenue data sets. Journal of Statistics and Applications, 2(1), 35-58.
20. Elsayed, H. A. H. and Yousof, H. M. (2019). The Burr X Nadarajah Haghighi distribution: statistical properties and application to the exceedances of flood peaks data. Journal of Mathematics and Statistics, 15, 146-157.
21. Elsayed, H. A. H. and Yousof, H. M. (2020). The generalized odd generalized exponential Fréchet model: univariate, bivariate and multivariate extensions with properties and applications to the univariate version. Pakistan Journal of Statistics and Operation Research, 529-544.
22. Elsayed, H. A. H. and Yousof, H. M. (2021). Extended Poisson Generalized Burr XII Distribution. Journal of Applied Probability and Statistics, 16(1), 01-30.
23. Emam, W.; Tashkandy, Y.; Goual, H.; Hamida, T.; Hiba, A.; Ali, M.M.; Yousof, H.M.; Ibrahim, M. (2023a) A New One-Parameter Distribution for Right Censored Bayesian and Non-Bayesian Distributional Validation under Various Estimation Methods. Mathematics 2023, 11, 897. https://doi.org/10.3390/math11040897
24. Emam, W.; Tashkandy, Y.; Hamedani, G.G.; Shehab, M.A.; Ibrahim, M.; Yousof, H.M. (2023b) A Novel Discrete Generator with Modeling Engineering, Agricultural and Medical Count and Zero-Inflated Real Data with Bayesian, and Non-Bayesian Inference. Mathematics 2023, 11, 1125. https://doi.org/10.3390/math1105112
25. Cordeiro, G. M., Afify, A. Z., Yousof, H. M., Pescim, R. R. and Aryal, G. R. (2017). The exponentiated Weibull-H family of distributions: Theory and Applications. Mediterranean Journal of Mathematics, 14(4), 155.
26. Goual, H. and Yousof, H. M. (2020). Validation of Burr XII inverse Rayleigh model via a modified chi-squared goodness-of-fit test. Journal of Applied Statistics, 47(3), 393-423.
27. Ibrahim. M., Aidi, K., Ali, M. M. and Yousof, H. M. (2021). The Exponential Generalized Log-Logistic Model: Bagdonavičius-Nikulin test for Validation and Non-Bayesian Estimation Methods. Communications for Statistical Applications and Methods, 29(1), 681–705.
28. Ibrahim, M., Ali, M. M., Goual, H. and Yousof, H. M. (2022). Censored and uncensored validation for the double Burr XII model using a new Nikulin-Rao-Robson goodness-of-fit test with Bayesian and non-Bayesian estimation, Pakistan Journal of Statistics and Operation Research, 18(4), 2022.
29. Ibrahim, M.; Emam, W.; Tashkandy, Y.; Ali, M.M.; Yousof, H.M. (2023) Bayesian and Non-Bayesian Risk Analysis and Assessment under Left-Skewed Insurance Data and a Novel Compound Reciprocal Rayleigh Extension. Mathematics 2023, 11, 1593. https://doi.org/10.3390/ math11071593

30. Ibrahim, M., Yadav, A. S., Yousof, H. M., Goual, H. and Hamedani, G. G. (2019). A new extension of Lindley distribution: modified validation test, characterizations and different methods of estimation. Communications for Statistical Applications and Methods, 26(5), 473-495.
31. Khedr, A. M., Nofal, Z. M., El Gebaly, Y. M. and Yousof, H. M. A Novel Family of Compound Probability Distributions: Properties, Copulas, Risk Analysis and Assessment under a Reinsurance Revenues Data Set. Thailand Statistician, forthcoming.
32. Khalil, M. G., Hamedani, G. G. and Yousof, H. M. (2019). The Burr X exponentiated Weibull model: Characterizations, mathematical properties and applications to failure and survival times data. Pakistan Journal of Statistics and Operation Research, 141-160.
33. Khalil, M. G., Yousof, H. M., Aidi, K., Ali, M. M., Butt, N. S. and Ibrahim. M. (2023). Modified Bagdonavicius-Nikulin Goodness-of-fit Test Statistic for the Compound Topp Leone Burr XII Model with Various Censored Applications. Statistics, Optimization & Information Computing, forthcoming.
34. Khalil, M. G., Yousof, H. M., Aidi, K., Ali, M. M., Butt, N. S. and Ibrahim. M. (2023). Modified Bagdonavicius-Nikulin Goodness-of-fit Test Statistic for the Compound Topp Leone Burr XII Model with Various Censored Applications. Statistics, Optimization & Information Computing, forthcoming.
35. Korkmaz, M. Ç., Alizadeh, M., Yousof, H. M. and Butt, N. S. (2018a). The generalized odd Weibull generated family of distributions: statistical properties and applications. Pakistan Journal of Statistics and Operation Research, 541-556.
36. Korkmaz, M. Ç., Yousof, H. M., Hamedani, G. G. and Ali, M. M. (2018b). The Marshall-Olkin generalized G Poisson family of distributions. Pak. J. Statist, 34(3), 251-267.
37. Lee, E. T. and Wang, J. (2003). Statistical methods for survival data analysis (Vol. 476). John Wiley & Sons.
38. Mansour, M. M., Ibrahim, M., Aidi, K., Butt, N. S., Ali, M. M., Yousof, H. M. and Hamed, M. S. (2020a). A New Log-Logistic Lifetime Model with Mathematical Properties, Copula, Modified Goodness-of-Fit Test for Validation and Real Data Modeling. Mathematics, 8(9), 1508.
39. Mansour, M. M., Butt, N. S., Ansari, S. I., Yousof, H. M., Ali, M. M. and Ibrahim, M. (2020b). A new exponentiated Weibull distribution's extension: copula, mathematical properties and applications. Contributions to Mathematics, 1 (2020) 57–66. DOI: 10.47443/cm.2020.0018
40. Mansour, M., Korkmaz, M. Ç., Ali, M. M., Yousof, H. M., Ansari, S. I. and Ibrahim, M. (2020c). A generalization of the exponentiated Weibull model with properties, Copula and application. Eurasian Bulletin of Mathematics, 3(2), 84-102.
41. Mansour, M., Rasekhi, M., Ibrahim, M., Aidi, K., Yousof, H. M. and Elrazik, E. A. (2020d). A New Parametric Life Distribution with Modified Bagdonavičius–Nikulin Goodness-of-Fit Test for Censored Validation, Properties, Applications, and Different Estimation Methods. Entropy, 22(5), 592.
42. Mansour, M., Yousof, H. M., Shehata, W. A. M. and Ibrahim, M. (2020e). A new two parameter Burr XII distribution: properties, copula, different estimation methods and modeling acute bone cancer data. Journal of Nonlinear Science and Applications, 13(5), 223-238.
43. Mansour, M. M., Butt, N. S., Yousof, H. M., Ansari, S. I. and Ibrahim, M. (2020f). A Generalization of Reciprocal Exponential Model: Clayton Copula, Statistical Properties and Modeling Skewed and Symmetric Real Data Sets. Pakistan Journal of Statistics and Operation Research, 16(2), 373-386.
44. Murthy, D.N.P., Xie, M. and Jiang, R. (2004). Weibull Models. John Wiley and Sons, Hoboken, New Jersey.
45. Rinne, H. (2009). The Weibull Distribution: A Handbook. CRC Press, Boca Raton, Florida.
46. Smith, R.L. AND J. NAYLOR, (1987). A comparison of maximum likelihood and Bayesian estimators for the three-parameter Weibull distribution. Journal of the Royal Statistical Society: Series C, 36(3) 358-369.
47. Refaie, M. K. A. (2018). Extended Poisson-exponentiated Weibull distribution: theoretical and computational aspects. pak. j. statist, 34(6), 513-530.
48. Refaie, M. K. A. (2019). A new two-parameter exponentiated Weibull model with properties and applications to failure and survival times. International Journal of Mathematical Archive, 10(2), 1-13.
49. Saber, M. M., Hamedani, G. G., Yousof, H. M. But, N. S., Ahmed, B. and Ibrahim, M. (2022) A Family of Continuous Probability Distributions: Theory, Characterizations, Properties and Different Copulas, CRC Press, Taylor & Francis Group.

50. Shehata, W. A. M. and Yousof, H. M. (2022). A novel two-parameter Nadarajah-Haghighi extension: properties, copulas, modeling real data and different estimation methods. Statistics, Optimization & Information Computing, 10(3), 725-749.
51. Shehata, W. A. M. and Yousof, H. M. (2021). The four-parameter exponentiated Weibull model with Copula, properties and real data modeling. Pakistan Journal of Statistics and Operation Research, 17(3), 649-667.
52. Shehata, W. A. M., Yousof, H. M. and Aboraya, M. (2021). A Novel Generator of Continuous Probability Distributions for the Asymmetric Left-skewed Bimodal Real-life Data with Properties and Copulas . Pakistan Journal of Statistics and Operation Research, 17(4), 943-961.
53. Shehata, W. A. M., Butt, N. S., Yousof, H. and Aboraya, M. (2022). A New Lifetime Parametric Model for the Survival and Relief Times with Copulas and Properties. Pakistan Journal of Statistics and Operation Research, 18(1), 249-272.
54. Tashkandy, Y., Emam, W., Ali, M. M., Yousof, H. M., Ahmed, B. (2023). Quality Control Testing with Experimental Practical Illustrations under the Modified Lindley Distribution Using Single, Double, and Multiple Acceptance Sampling Plans. Mathematics. 2023; 11(9):2184. https://doi.org/10.3390/math11092184
55. Yadav, A. S., Shukla, S., Goual, H., Saha, M. and Yousof, H. M. (2022). Validation of xgamma exponential model via Nikulin-Rao-Robson goodness-of- fit test under complete and censored sample with different methods of estimation. Statistics, Optimization & Information Computing, 10(2), 457-483.
56. Yousof, H. M., Afify, A. Z., Cordeiro, G. M., Alzaatreh, A. and Ahsanullah, M. (2017a). A New Four-Parameter Weibull Model for Lifetime Data. Journal of Statistical Theory and Applications, 16(4), 448-466.
57. Yousof, H. M., Ali, M. M., Hamedani, G. G., Aidi, K. & Ibrahim, M. (2022). A new lifetime distribution with properties, characterizations, validation testing, different estimation methods. Statistics, Optimization & Information Computing, 10(2), 519-547.
58. Yousof, H. M., Ansari, S. I., Tashkandy, Y., Emam, W., Ali, M. M., Ibrahim, M., Alkhayyat, S. L. (2023a). Risk Analysis and Estimation of a Bimodal Heavy-Tailed Burr XII Model in Insurance Data: Exploring Multiple Methods and Applications. Mathematics. 2023; 11(9):2179. https://doi.org/10.3390/math11092179
59. Yousof, H.M.; Emam, W.; Tashkandy, Y.; Ali, M.M.; Minkah, R.; Ibrahim, M. (2023b) A Novel Model for Quantitative Risk Assessment under Claim-Size Data with Bimodal and Symmetric Data Modeling. Mathematics 2023, 11, 1284. https://doi.org/10.3390/math11061284
60. Yousof, H. M., Rasekhi, M., Afify, A. Z., Ghosh, I., Alizadeh, M. and Hamedani, G. G. (2017b). The beta Weibull-G family of distributions: theory, characterizations and applications. Pakistan Journal of Statistics, 33(2).
61. Yousof, H.M.; Tashkandy, Y.; Emam, W.; Ali, M.M.; Ibrahim, M. (2023c) A New Reciprocal Weibull Extension for Modeling Extreme Values with Risk Analysis under Insurance Data. Mathematics 2023, 11, 966.
62. Weibull, W., (1951). Wide applicability. Journal of applied mechanics. 103(730): p. 293-297.